REACTOR VESSEL MATERIAL SURVEILLANCE PROGRAM FOR DONALD C. COOK UNIT NO. 2 ANALYSIS OF CAPSULE T

by
E. B. Norris

FINAL REPORT
SwRI Project No. 02-5928

for
Indiana & Michigan Power Company
Donald C. Cook Nuclear Plant
Bridgman, Michigan 49106

September 16, 1981

SOUTHWEST RESEARCH INSTITUTE
SAN ANTONIO HOUSTON

SOUTHWEST RESEARCH INSTITUTE
Post Office Drawer 28510, 6220 Culebra Road
San Antonio, Texas 78284

REACTOR VESSEL MATERIAL SURVEILLANCE PROGRAM FOR DONALD C. COOK UNIT NO. 2 ANALYSIS OF CAPSULE T

by

E. B. Norris

FINAL REPORT
SwRI Project No. 02-5928

J R Jensen DATE 11/16/81

for

Indiana & Michigan Power Company
Donald C. Cook Nuclear Plant
Bridgman, Michigan 49106

September 16, 1981

Approved:

U. S. Lindholm, Director
Department of Materials Sciences

ABSTRACT

The first vessel material surveillance capsule removed from the Donald C. Cook Unit No. 2 nuclear power plant has been tested, and the results have been evaluated. Heatup and cooldown limit curves for normal operation have been developed for up to 12 and 32 effective full power years of operation.

TABLE OF CONTENTS

LIST OF FIGURES

LIST OF TABLES

I. SUMMARY OF RESULTS AND CONCLUSIONS

The analysis of the first material surveillance capsule removed from The Donald C. Cook Unit No. 2 reactor pressure vessel led to the following conclusions:

(1) Based on a calculated neutron spectral distribution, Capsule T received a fast fluence of 2.2×10^{18} neutrons/cm^2 (E > 1 MeV).

(2) The surveillance specimens of the core beltline materials experienced shifts in transition temperature of 40°F to 80°F as a result of the above exposure.

(3) The intermediate shell plate materials exhibited the largest shift in RT_{NDT} and will control the heatup and cooldown limitations throughout the design lifetime of the pressure vessel.

(4) The estimated maximum neutron fluence of 6.7×10^{17} neutrons/cm^2 (E > 1 MeV) received by the vessel wall accrued in 1.08 effective full power years (EFPY). Therefore, the projected maximum neutron fluence after 32 EFPY is 2.0×10^{19} neutrons/cm^2 (E > 1 MeV). This estimate is based on a lead factor of 3.24 between the center of Capsule T and the point of maximum pressure vessel flux.

(5) Based on Regulatory Guide 1.99 trend curves, the projected maximum shift in ductile-brittle transition temperature of the Donald C. Cook Unit 2 vessel core beltline plates at the 1/4T and 3/4T positions after 12 EFPY of operation are 168°F and 113°F, respectively. These values were used as the bases for computing heatup and cooldown limit curves for up to 12 EFPY of operation.

(6) The maximum shifts in the transition temperature of the Donald C. Cook Unit 2 vessel core beltline plates at the 1/4T and 3/4T positions after 32 EFPY of operation are projected to be 240°F and 149°F, respectively. These values were used as the bases for computing heatup and cooldown limit curves for up to 32 EFPY of operation.

(7) The Donald C. Cook Unit No. 2 vessel plates, weld metal, and HAZ material located in the core beltline region are projected to retain sufficient toughness to meet the current requirements of 10CFR50 Appendix G throughout the design life of the unit.

II. BACKGROUND

The allowable loadings on nuclear pressure vessels are determined by applying the rules in Appendix G, "Fracture Toughness Requirements," of 10CFR50 [1]. In the case of pressure-retaining components made of ferritic materials, the allowable loadings depend on the reference stress intensity factor (K_{IR}) curve indexed to the reference nil ductility temperature (RT_{NDT}) presented in Appendix G, "Protection Against Non-ductile Failure," of Section III of the ASME Code [2]. Further, the materials in the beltline region of the reactor vessel must be monitored for radiation-induced changes in RT_{NDT} per the requirements of Appendix H, "Reactor Vessel Material Surveillance Program Requirements," of 10CFR50.

The RT_{NDT} is defined in paragraph NB-2331 of Section III of the ASME Code as the highest of the following temperatures:

(1) Drop-weight Nil Ductility Temperature (DW-NDT) per ASTM E 208 [3];

(2) 60 deg F below the 50 ft-lb Charpy V-notch (C_V) temperature;

(3) 60 deg F below the 35 mil C_V temperature.

The RT_{NDT} must be established for all materials, including weld metal and heat-affected zone (HAZ) material as well as base plates and forgings, which comprise the reactor coolant pressure boundary.

It is well established that ferritic materials undergo an increase in strength and hardness and a decrease in ductility and toughness when exposed to neutron fluences in excess of 10^{17} neutrons per cm^2 (E > 1 MeV) [4]. Also, it has been established that tramp elements, particularly

copper and phosphorus, affect the radiation embrittlement response of ferritic materials [5-6]. The relationship between increase in RT_{NDT} and copper content is defined in Regulatory Guide 1.99. Although this document is being revised by the NRC to reflect a more recent evaluation of neutron embrittlement data by the Metal Properties Council [7], estimates of shifts in RT_{NDT} in this report are based on the current Revision 1 of Regulatory Guide 1.99 [8].

In general, the only ferritic pressure boundary materials in a nuclear plant which are expected to receive a fluence sufficient to affect RT_{NDT} are those materials which are located in the core beltline region of the reactor pressure vessel. Therefore, material surveillance programs include specimens machined from the plate or forging material and weldments which are located in the core beltline region of high neutron flux density. ASTM E 185 [9] describes the recommended practice for monitoring and evaluating the radiation-induced changes occurring in the mechanical properties of pressure vessel beltline materials.

Westinghouse has provided such a surveillance program for the Donald C. Cook Unit No. 2 nuclear power plant. The encapsulated C_v specimens are located on the O.D. surface of the thermal shield where the fast neutron flux density is about three times that at the adjacent vessel wall surface. Therefore, the increases (shifts) in transition temperatures of the materials in the pressure vessel are generally less than the corresponding shifts observed in the surveillance specimens. However, because of azimuthal variations in neutron flux density, capsule fluences may lead or lag the maximum vessel fluence in a corresponding exposure period. The capsules also contain several dosimeter materials

for experimentally determining the average neutron flux density at each capsule location during the exposure period.

The Donald C. Cook Unit No. 2 material surveillance capsules also include tensile specimens as recommended by ASTM E 185. At the present time, irradiated tensile properties are used only to indicate that the materials tested continue to meet the requirements of the appropriate material specification. In addition, the material surveillance capsules contain wedge opening loading (WOL) fracture mechanics specimens. Current technology limits the testing of these specimens at temperatures well below the minimum service temperature to obtain valid fracture mechanics data per ASTM E 399 [10], "Standard Method of Test for Plane-Strain Fracture Toughness of Metallic Materials." However, recent work reported by Mager and Witt [11] may lead to methods for evaluating high-toughness materials with small fracture mechanics specimens. Currently, the NRC suggests storing these specimens until an acceptable testing procedure has been defined.

This report describes the results obtained from testing the contents of Capsule T. These data are analyzed to estimate the radiation-induced changes in the mechanical properties of the pressure vessel at the time of the refuelling outage as well as predicting the changes expected to occur at selected times in the future operation of the Donald C. Cook Unit No. 2 power plant.

III. DESCRIPTION OF MATERIAL SURVEILLANCE PROGRAM

The Donald C. Cook Unit No. 2 material surveillance program is described in detail in WCAP 8512 [12], dated November 1975. Eight materials surveillance capsules were placed in the reactor vessel between the thermal shield and the vessel wall prior to startup, see Figure 1. The vertical center of each capsule is opposite the vertical center of the core. The Capsule T neutron flux density was initially reported to lead the maximum flux density on the vessel I.D. by a factor of 2.9 [12]. However, in a letter to the American Electric Power Service Corporation [13], Westinghouse reported that the 40° capsule lead factor had been changed to 3.7 as a result of refined calculational methods.

The capsules each contain Charpy V-notch, tensile, and WOL specimens machined from the SA533 Gr B, Cl 1 plate, weld metal, and heat-affected zone (HAZ) materials located at the core beltline. The chemistries and heat treatments of the vessel surveillance materials are summarized in Table I. All test specimens were machined from the test materials at the quarter-thickness (1/4 T) location after performing a simulated postweld stress-relieving treatment. Weld and HAZ specimens were machined from a stress-relieved weldment which joined sections of the intermediate and lower shell plates. HAZ specimens were obtained from the plate C5521-2 side of the weldment. The longitudinal base metal C_v specimens were oriented with their long axis parallel to the primary rolling direction and with V-notches perpendicular to the major plate surfaces. The transverse base metal C_v specimens were oriented with their long axis perpendicular to the primary rolling direction and with V-notches perpendicular to the

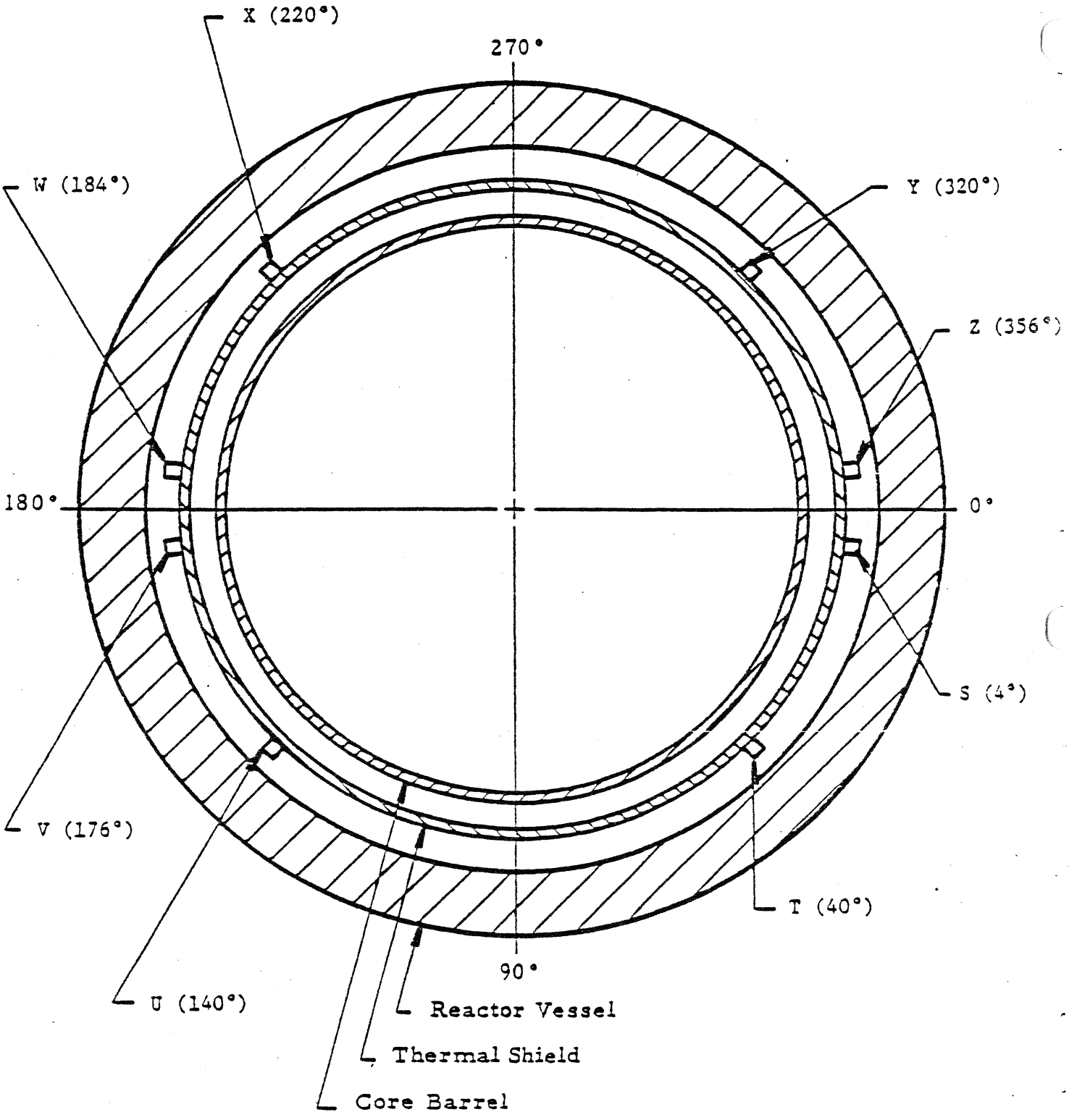

FIGURE 1. ARRANGEMENT OF SURVEILLANCE CAPSULES IN THE PRESSURE VESSEL

TABLE I

DONALD C. COOK UNIT NO. 2 REACTOR VESSEL SURVEILLANCE MATERIALS [14]

Heat Treatment History

Shell Plate Material:

Heated to 1700 ± 50°F for 4-1/2 hours, water quenched;
Heated to 1600 ± 50°F for 5 hours, water quenched;
Tempered at 1250 ± 50°F for 4-1/2 hours, air cooled;
Stress relieved at 1150 ± 25°F for 51-1/2 hours, furnace cooled.

Weldment:

Stress relieved at 1140 ± 25°F for 9 hours, furnace cooled.

Chemical Composition (Percent)

Material	C	Mn	P	S	Si	Ni	Mo	Cu	Cr
Plate C5521-2 (a)	0.21	1.29	0.013	0.015	0.16	0.58	0.50	0.14	-
Plate C5521-2 (b)	0.220	1.280	0.017	0.014	0.270	0.580	0.550	0.110	0.072
Weld Metal (c)	0.08	1.42	0.019	0.016	0.36	0.96	-	0.05	0.07
Weld Metal (b)	0.110	1.330	0.022	0.012	0.440	0.970	0.540	0.055	0.068

(a) Lukens Steel analysis
(b) Westinghouse analysis
(c) Chicago Bridge and Iron analysis

major plate surfaces. Tensile specimens were machined with the longitudinal axis perpendicular to the plate primary rolling direction. The WOL specimens were machined with the simulated crack parallel to the primary rolling direction and perpendicular to the major plate surfaces. All mechanical test specimens, see Figure 2, were taken at least one plate thickness from the quenched edges of the plate material.

Capsule T contained 44 Charpy V-notch specimens (8 longitudinal and 12 transverse from the plate material, plus 12 each from weld metal and HAZ material); 4 tensile specimens (2 plate and 2 weld metal); and 4 WOL specimens (either plate or weld metal). The specimen numbering system and location within Capsule T is shown in Figure 3.

Capsule T also was reported to contain the following dosimeters for determining the neutron flux density:

Target Element	Form	Quantity
Iron	Bare wire	5
Copper	Bare wire	3
Nickel	Bare wire	3
Cobalt (in aluminum)	Bare wire	2
Cobalt (in aluminum)	Cd shielded wire	2
Uranium-238	Cd shielded oxide	1
Neptunium-237	Cd shielded oxide	1

Two eutectic alloy thermal monitors had been inserted in holes in the steel spacers in Capsule T. One (located at the bottom) was 2.5% Ag and 97.5% Pb with a melting point of 579°F. The other (located at the top of the capsule) was 1.75% Ag, 0.75% Sn, and 97.5% Pb having a melting point of 590°F.

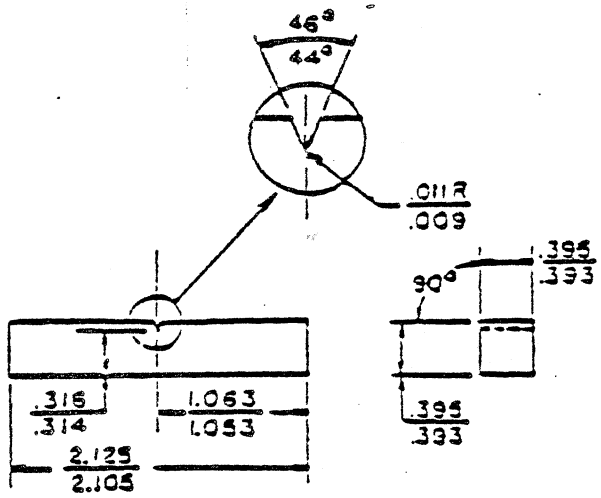

(a) Charpy V-Notch Impact Specimen

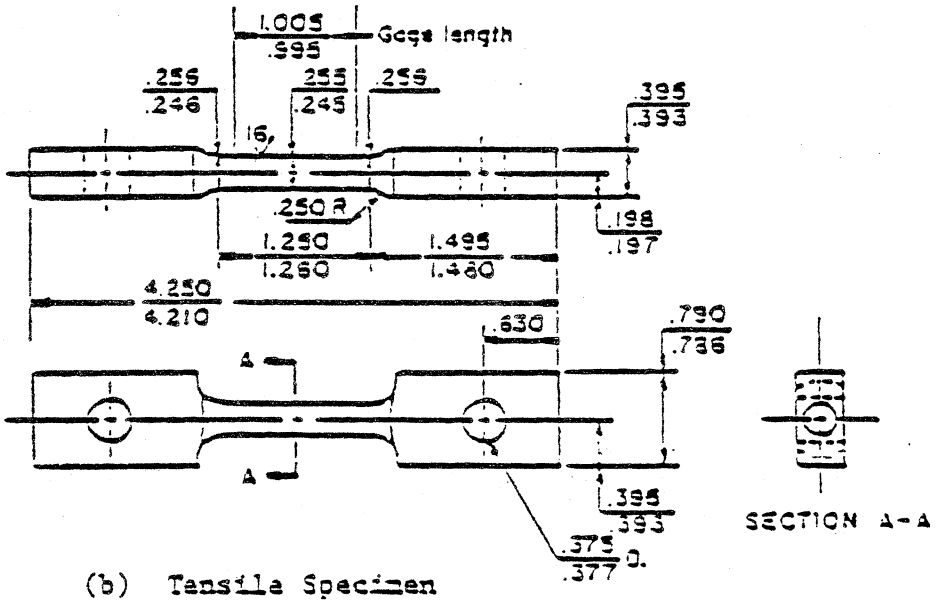

(b) Tensile Specimen

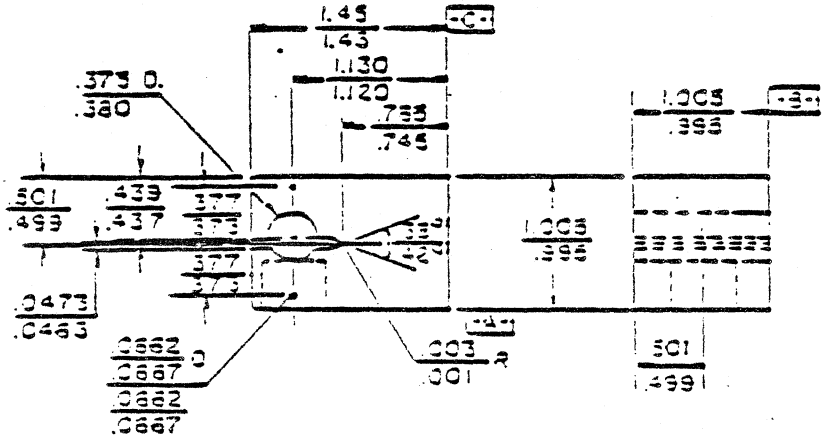

(c) Wedge Opening Loading Specimen

FIGURE 2. VESSEL MATERIAL SURVEILLANCE SPECIMENS

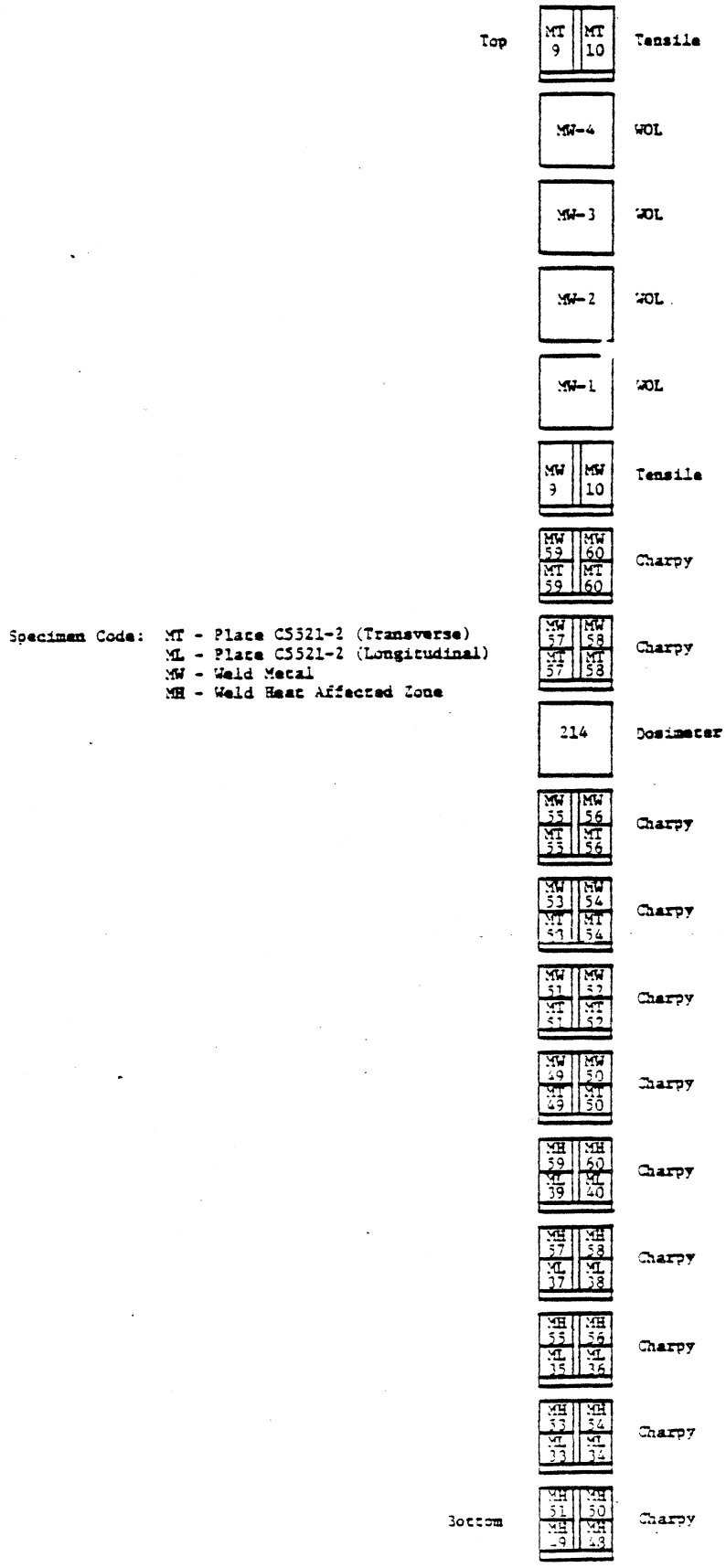

FIGURE 3. ARRANGEMENT OF SPECIMENS AND DOSIMETERS IN CAPSULE T

IV. TESTING OF SPECIMENS FROM CAPSULE T

The capsule shipment, capsule opening, specimen testing, and reporting of results were carried out in accordance with the Project Plan for Donald C. Cook Unit No. 2 Reactor Vessel Irradiation Surveillance Program. The SwRI Nuclear Projects Operating Procedures called out in this plan include:

(1) XIII-MS-104-0, "Shipment of Westinghouse PWR Vessel Material Surveillance Capsule Using SwRI Cask and Equipment"

(2) XI-MS-101-0, "Determination of Specific Activity and Analysis of Radiation Detector Specimens"

(3) XI-MS-103-0, "Conducting Tension Tests on Metallic Specimens"

(4) XI-MS-104-0, "Charpy Impact Tests on Metallic Specimens"

(5) XIII-MS-103-0, "Opening Radiation Surveillance Capsules and Handling and Storing Specimens"

(6) XI-MS-5-0, "Conducting Wedge-Opening-Loading Tests on Metallic Materials"

Copies of the above documents are on file at SwRI.

A. Shipment, Opening, and Inspection of Capsule

Southwest Research Institute utilized Procedure XIII-MS-104-0 for the shipment of Capsule T to the SwRI laboratories. SwRI personnel severed the capsule from its extension tube, sectioned the extension tube into several lengths, supervised the loading of the capsule and extension tube materials into the shipping cask, and transported the cask to San Antonio, Texas.

The capsule was opened and the contents identified and stored in rdance with Procedure XIII-MS-103-0. The long seam welds were milled in a hot cell using a Bridgeport vertical milling machine. Before ing the long seam weld beads, transverse saw cuts were made to remove capsule ends. After the long seam welds had been milled off, the top of the capsule shell was removed. The specimens and spacer blocks carefully removed and placed in indexed receptacles, identifying each ule location. After the disassembly had been completed, each specimen carefully checked to insure agreement with the identification and tion as listed in WCAP 8512 [12]. No discrepancies were found.

The thermal monitors and neutron dosimeter wires were removed from holes in the spacers. The thermal monitors, contained in quartz s, were examined. No evidence of melting was observed, thus indicating the maximum temperature during exposure of Capsule T did not exceed F. The top and bottom Cd-covered Co-Al neutron monitors were not in capsule, but all other neutron dosimeters were correctly accounted for. lack of Cd-covered Co-Al dosimeters had no significant impact on the eillance program because they were intended for the determination of thermal neutron flux and thermal flux burnup corrections are not needed WR programs.

Neutron Dosimetry

The gamma activities of the dosimeters were determined in accordance Procedure XI-MS-101-0 using an IT-5400 multichannel analyzer and a (Li) coaxial detector system. The calibration of the equipment was mplished with ^{54}Mn, ^{60}Co, and ^{137}Cs radioactivity standards obtained the U.S. Department of Commerce National Bureau of Standards. All ivities were corrected to the time-of removal (TOR) at reactor shutdown.

The dosimeter wires were weighed on a Mettler microbalance, and the fission monitors were weighed on a Mettler digital balance after these materials had been deencapsulated. Infinitely dilute saturated activities (A_{SAT}) were calculated for each of the dosimeters because A_{SAT} is directly related to the product of the energy-dependent microscopic activation cross section and the neutron flux density. The relationship between A_{TOR} and A_{SAT} is given by:

$$\frac{A_{TOR}}{A_{SAT}} = \sum_{m=1}^{m=n} \left(1 - e^{-\lambda T_m}\right)\left(e^{-\lambda t_m}\right)$$

where: λ = decay constant for the activation product, day^{-1};

T_m = equivalent operating days at 3391 MwTh for operating period m; and

t_m = decay time after operating period m, days.

An alternate expression which gives equivalent results is:

$$\frac{A_{TOR}}{A_{SAT}} = \sum_{m=1}^{m=n} P_m\left(1 - e^{-\lambda T_o}\right)\left(e^{-\lambda t_m}\right)$$

where: T_o = operating days; and

P_m = average fraction of full power during operating period.

The Donald C. Cook Unit No. 2 operating history up to the 1979 refueling shutdown, which was used in the calculation of A_{TOR}, is presented in Table II.

The primary result desired from the dosimeter analysis is the total fast neutron fluence (> 1 MeV) which the surveillance specimens received. The average flux density at full power is given by:

TABLE II

SUMMARY OF REACTOR OPERATIONS
DONALD C. COOK UNIT NO. 2

Operating Period	Dates Start	Dates Stop	Operating Days	Shutdown Days	Power Generation (MWD_t)	Equivalent Operating Days (T_m)(a)	Decay Time After Period (t_m)
1	03/22/78	04/19/78	33	-	23,969	7.07	549
	04/20/78	05/02/78	-	14	-	-	-
2	05/03/78	05/19/78	17	-	27,264	8.04	518
	05/20/78	05/31/78	-	12	-	-	-
3	06/01/78	06/03/78	3	-	5,510	1.62	503
	06/04/78	06/04/78	-	1	-	-	-
4	06/05/78	07/21/78	47	-	103,423	30.50	455
	07/22/78	08/04/78	-	14	-	-	-
5	08/05/78	08/21/78	17	-	51,223	15.11	424
	08/22/78	08/22/78	-	1	-	-	-
6	08/23/78	08/28/78	6	-	12,543	3.70	417
	08/29/78	09/01/78	-	4	-	-	-
7	09/02/78	11/09/78	69	-	206,496	60.90	344
	11/10/78	11/23/78	-	14	-	-	-
8	11/24/78	04/07/79	135	-	423,785	124.97	195
	04/08/79	04/08/79	-	1	-	-	-
9	04/09/79	05/19/79	41	-	132,362	39.03	153
	05/20/79	07/02/79	-	44	-	-	-
10	07/03/79	10/19/79	109	-	356,918	105.25	0
				Total Cycle 1 -	1,343,493	396.19(b)	

(a) One equivalent operating day = 3391 MW_t
(b) Equals 1.08 EFPY

$$\phi = \frac{A_{SAT}}{N_0 \bar{\sigma}}$$

where: ϕ = energy-dependent neutron flux density, n/cm^2-sec;

A_{SAT} = saturated activity, dps/mg target element;

$\bar{\sigma}$ = spectrum-averaged activation cross section, cm^2; and

N_0 = number of target atoms per mg.

The total neutron fluence is then equal to the product of the average neutron flux density and the equivalent reactor operating time at full power.

In Capsule T, all 12 weld metal and all but two of the 12 HAZ Charpy specimens were located in the specimen layer nearest to the vessel wall, and the vessel plate (longitudinal and transverse) Charpy specimens were located in the specimen layer nearest to the core. Since there is a radial dependence of the fast neutron flux in the vessel, the neutron exposure received by the weld metal and HAZ Charpy specimens is expected to be lower than that received by the vessel plate Charpy specimens. The dosimetry program was planned to provide information on the radial dependence of the fast flux since the copper and nickel threshold detectors were located on the radial centerlines of the Charpy specimen layers nearest to and farthest from the core, respectively, and the iron threshold detectors were located at the radial position corresponding to the interface between the two Charpy specimen layers. Additional dosimetry included the fission monitors located at the radial centerline of the capsule and the bare cadium-shielded cobalt-aluminum monitors located at the radial centerline of the Charpy specimen layer nearest the pressure vessel wall.

A discrete ordinates Sn transport analysis for the Donald C. Cook Unit No. 2 reactor vessel was performed to determine the axial, radial, and azimuthal dependence of the fast neutron (E > 1.0 MeV) flux density and energy spectrum within the reactor vessel and surveillance capsules. These results were used to calculate the spectrum-averaged cross-sections for the threshold detectors and the lead factors for use in relating neutron exposure of the pressure vessel to that of the surveillance capsule. The pertinent factors obtained from this transport analysis are summarized in Table III. The 3.24 center-of-capsule lead factor agrees well with the revised 3.7 average lead factor reported by Westinghouse [13].

The Capsule T dosimetry results are presented in Table IV. A summary of the capsule and vessel I.D. fluxes calculated for full-power operation is as follows:

Dosimeter Type	Measured Capsule Flux $cm^{-2} \cdot sec^{-1}$, E > 1 MeV	Lead Factor	Peak Vessel Flux at I.D. $cm^{-2} \cdot sec^{-1}$, E > 1 MeV
Copper	5.64×10^{10}	3.38	1.67×10^{10}
Fission	7.80×10^{10}	3.24	2.41×10^{10}
Iron	5.56×10^{10}*	3.02	1.84×10^{10}
Nickel	5.25×10^{10}	2.71	1.94×10^{10}

* If a fission-spectrum energy distribution is assumed at the capsule location, the cross-section for the $^{54}Fe(n,p)^{54}Mn$ reaction (E > 1.0 MeV) would be 98.26 mb [4], and the resulting value for fast flux at the capsule location would be 4.88×10^{10} $cm^{-2} \cdot sec^{-1}$. This value is reported for reference only and has not been used in the analysis of results.

The discrepancies in the peak vessel flux values determined from the several dosimeter materials are attributed primarily to the uncertainties in

TABLE III

RESULTS OF DISCRETE ORDINATES Sn TRANSPORT ANALYSIS
DONALD C. COOK UNIT NO. 2
CAPSULE T

A. Calculated Reaction Cross-Sections for Analysis of Fast Neutron Monitors (E > 1.0 MeV)

Reaction	$\bar{\sigma}$ (barns)
$^{54}Fe(n,p)^{54}Mn$	.0863
$^{58}Ni(n,p)^{58}Co$	.115
$^{63}Cu(n,\alpha)^{60}Co$	.00093
$^{238}U(n,f)$	.385
$^{237}Np(n,f)$	2.46

B. Calculated Capsule Lead Factors

Position[a]	Location within Capsule	Lead Factor[b]
211.7 cm	Center of core-side Charpy layer	3.38
211.9 cm	Center of capsule	3.24
212.2 cm	Center of two specimen layers	3.02
212.7 cm	Center of vessel-side Charpy layer	2.71

(a) Distance from center of core

(b) $\frac{\text{Capsule neutron flux density, E > 1.0 MeV}}{\text{Maximum neutron flux density at vessel I.D., E > 1.0 MeV}}$

TABLE IV

SUMMARY OF NEUTRON DOSIMETRY RESULTS
DONALD C. COOK UNIT NO. 2, CAPSULE T

Dosimeter Position[a]	Dosimeter Identification	Activation Reaction	A_{TOR} (dps/mg)	A_{SAT} (dps/mg)	Capsule Flux, ϕ, E > 1.0 MeV[b] $cm^{-2} \cdot sec^{-1}$
211.7 cm	Cu (Top Middle)	$^{63}Cu(n,\alpha)^{60}Co$	4.53×10^{1}	3.47×10^{2}	5.69×10^{10}
↓	Cu (Middle)	↓	4.43×10^{1}	3.39×10^{2}	5.56×10^{10}
↓	Cu (Bottom Middle)	↓	4.51×10^{1}	3.46×10^{2}	5.67×10^{10}
				Average =	5.64×10^{10}
211.9 cm	U-238 (Middle)	$^{238}U(n,f)^{137}Cs$	1.06×10^{2}	4.30×10^{3}	7.36×10^{10}
↓	Np-237 (Middle)	$^{237}Np(n,f)^{137}Cs$	8.22×10^{2}	3.35×10^{4}	8.24×10^{10}
				Average =	7.80×10^{10}
212.2 cm	Fe (Top)	$^{54}Fe(n,p)^{54}Mn$	1.59×10^{3}	2.97×10^{3}	5.50×10^{10}
↓	Fe (Top Middle)	↓	1.62×10^{3}	3.03×10^{3}	5.61×10^{10}
↓	Fe (Middle)	↓	1.57×10^{3}	2.94×10^{3}	5.45×10^{10}
↓	Fe (Bottom Middle)	↓	1.63×10^{3}	3.06×10^{3}	5.66×10^{10}
↓	Fe (Bottom)	↓	1.60×10^{3}	3.00×10^{3}	5.56×10^{10}
				Average =	5.56×10^{10}
212.7 cm	Ni (Top Middle)	$^{58}Ni(n,p)^{58}Co$	3.59×10^{4}	4.27×10^{4}	5.30×10^{10}
↓	Ni (Middle)	↓	3.50×10^{4}	4.16×10^{4}	5.17×10^{10}
↓	Ni (Bottom Middle)	↓	3.57×10^{4}	4.24×10^{4}	5.27×10^{10}
				Average =	5.25×10^{10}
212.7 cm	Co (Top)	$^{59}Co(n,\gamma)^{60}Co$	4.96×10^{6}	3.80×10^{7}	(c)
↓	Co (Bottom)	↓	6.31×10^{6}	4.83×10^{7}	(c)

(a) Distance from center of core
(b) Calculated flux values subject to ± 16.5% uncertainty (1σ)
(c) Not applicable

the calculated spectra and in the reaction cross sections. Other neutronic factors contributing to the estimated ± 16.5% uncertainty (1σ) in a calculated flux value are the determination of disintegration rates and the calculation of reaction rates (A_{SAT}/N_0).

Averaging the results obtained from all Capsule T neutron dosimeters, the peak neutron flux incident of the I.D. surface of the pressure vessel during fuel cycle 1 is calculated to be 1.96×10^{10} $cm^{-2} \cdot sec^{-1}$, E > 1 MeV. The calculated full power neutron flux for the weld metal and HAZ Charpy specimen layer is given by:

$$1.96 \times 10^{10} \times 2.71 = 5.3 \times 10^{10}$$

Similarly, the calculated full power neutron flux for the vessel plate Charpy specimens, the tensile specimens, and the WOL specimens are given by:

$1.96 \times 10^{10} \times 3.38 = 6.6 \times 10^{10}$ (Plate C_V Specimens)

$1.96 \times 10^{10} \times 3.02 = 5.9 \times 10^{10}$ (Tensile Specimens)

$1.96 \times 10^{10} \times 3.24 = 6.4 \times 10^{10}$ (WOL Specimens)

Since Donald C. Cook Unit No. 2 operated for 396.19 effective full power days up to the October 1979 refueling, the calculated capsule and vessel fluences to that time are as follows:

- Weld Metal and HAZ Charpy Specimens - 1.8×10^{18} n/cm^2
- Vessel Plate Charpy Specimens - 2.3×10^{18} n/cm^2
- Tensile Specimens - 2.0×10^{18} n/cm^2
- WOL Specimens - 2.2×10^{18} n/cm^2
- Pressure Vessel ID Surface - 6.7×10^{17} n/cm^2

C. Mechanical Property Tests

The irradiated Charpy V-notch specimens were tested on a SATEC impact machine in accordance with Procedure XI-MS-104-0. The test temperatures were selected to develop the ductile-brittle transition and upper shelf regions. The unirradiated Charpy V-notch impact data reported by Westinghouse [12] and the data obtained by SwRI on the specimens contained in Capsule T are presented in Tables V through VIII. The Charpy V-notch transition curves for the two plate materials, the weld metal, and the HAZ material are presented in Figures 4 through 7. The radiation-induced shift in transition temperatures are indicated at the 50 ft-lb, 30 ft-lb, and 35 mil lateral expansion levels. A summary of the shifts in RT_{NDT} and C_v upper shelf energies for each material are presented in Table IX.

Tensile tests were carried out in accordance with Procedure XI-MS-103-0 using a 50-kip capacity tester equipped with a strain gage extensometer, load cell, and autographic recording equipment. Tensile tests on the plate material were run at 250°F and 550°F; those on the weld metal were run at 210°F and 550°F. The results, along with tensile data reported by Westinghouse on the unirradiated materials [12], are presented in Table X. The load-strain records are included in Appendix A.

Testing of the WOL specimens was deferred at the request of Indiana & Michigan Electric Company. The specimens are in storage at the SwRI radiation laboratory.

TABLE V

CHARPY V-NOTCH IMPACT TEST RESULTS, D.C. COOK UNIT NO. 2
VESSEL INTERMEDIATE SHELL PLATE C5521-2, LONGITUDINAL ORIENTATION

Condition	Specimen No.	Test Temperature (deg F)	Fracture Energy (ft-lb)	Lateral Expansion (mils)	Fracture Appearance (% shear)
Capsule T	ML-40	50	17	15	10
	ML-33	75	25	24	10
	ML-39	100	38.5	30	20
	ML-35	120	72.5	58	25
	ML-36	165	92	65	80
	ML-34	210	110	85	100
	ML-37	250	110	88	100
	ML-38	300	112	89	100
(a)	(b)	0	15	12	18
		0	18	13	19
		0	15	11	18
		25	26	20	30
		25	31	23	25
		25	43	29	25
		50	52	38	35
		50	47	37	35
		50	46	34	35
		70	65	47	42
		70	65	49	42
		70	76	54	55
		100	91	66	65
		100	98	76	70
		100	90	67	62
		125	126	78	85
		125	114	79	77
		125	103	70	75
		210	122	83	100
		210	132	86	100
		210	128	84	100

(a) Unirradiated [12]
(b) Not reported

TABLE VI

CHARPY V-NOTCH IMPACT TEST RESULTS, D.C. COOK UNIT NO. 2
VESSEL INTERMEDIATE SHELL PLATE C5521-2, TRANSVERSE ORIENTATION

Condition	Specimen No.	Test Temperature (deg F)	Fracture Energy (ft-lb)	Lateral Expansion (mils)	Fracture Appearance (% shear)
Capsule T	MT-60	20	10	9	Nil
	MT-49	75	20.5	18	5
	MT-56	75	17	18	10
	MT-57	100	38.5	35	10
	MT-51	120	37	32	20
	MT-58	120	32	31	20
	MT-52	165	54	49	30
	MT-59	165	47	46	30
	MT-50	210	66.5	66	80
	MT-53	250	76	71	100
	MT-54	300	75.5	70	100
	MT-55	300	71	68	100
(a)	(b)	-50	5.5	0	5
		-50	6	1	5
		-50	6	0	5
		10	39	27	29
		10	29	17	25
		10	25	18	30
		70	43	32	40
		70	42	33	43
		70	39	28	43
		100	66	47	60
		100	71.5	53	63
		100	68	49	65
		120	67.5	56	58
		120	76	60	65
		120	75	59	72
		210	81	64	100
		210	88	63	100
		210	90	66	100

(a) Unirradiated [12]
(b) Not reported

TABLE VII

CHARPY V-NOTCH IMPACT TEST RESULTS, D.C. COOK UNIT NO. 2
VESSEL CORE REGION WELD METAL

Condition	Specimen No.	Test Temperature (deg F)	Fracture Energy (ft-lb)	Lateral Expansion (mils)	Fracture Appearance (% shear)
Capsule T	MW-59	-25	12	11	5
	MW-58	20	21.5	20	15
	MW-57	50	23	21	10
	MW-60	60	35.5	32	30
	MW-49	75	58.5	48	75
	MW-56	75	46.5	44	95
	MW-51	120	49	44	20
	MW-52	165	77	69	100
	MW-50	210	75	75	100
	MW-53	250	68	55	100
	MW-54	300	74	72	100
	MW-55	300	75	63	100
(a)	(b)	-25	20	20	48
		-25	22	17	30
		-25	31.5	25	40
		20	32	24	38
		20	35	28	47
		20	33	27	50
		60	58	48	74
		60	47	37	65
		60	39	29	50
		100	74	63	95
		100	56	47	85
		100	65	53	95
		210	72	68	100
		210	70	63	100
		210	77	64	100
		300	72	66	98
		300	79	71	100
		300	81	70	100

(a) Unirradiated [12]
(b) Not reported

TABLE VIII

CHARPY V-NOTCH IMPACT TEST RESULTS, D.C. COOK UNIT NO. 2
VESSEL CORE REGION WELD HEAT-AFFECTED ZONE MATERIAL

Condition	Specimen No.	Test Temperature (deg F)	Fracture Energy (ft-lb)	Lateral Expansion (mils)	Fracture Appearance (% shear)
Capsule T	MH-59	-50	10	11	20
	MH-58	-25	22	20	30
	MH-60	0	38.5	32	50
	MH-57	20	43	32	60
	MH-56	50	97	68	90
	MH-49	75	92.5	60	90
	MH-51	120	125	80	95
	MH-52	165	104	66	100
	MH-50	210	62.5	56	100
	MH-53	250	110.5	69	100
	MH-54	300	112	72	100
	MH-55	300	110.5	70	100
(a)	(b)	-100	21	12	30
		-100	5	1	12
		-100	14	8	29
		-50	34	16	35
		-50	23	21	27
		-50	70.5	39	53
		-25	89	52	65
		-25	70	43	60
		-25	90	52	60
		0	95	59	70
		0	76	52	65
		0	130	75	100
		50	84	55	90
		50	67	48	85
		50	136	76	100
		125	95	66	95
		125	104	75	99
		125	82	71	90
		210	147	77	100
		210	113	80	100
		210	86	71	100

(a) Unirradiated [12]
(b) Not reported.

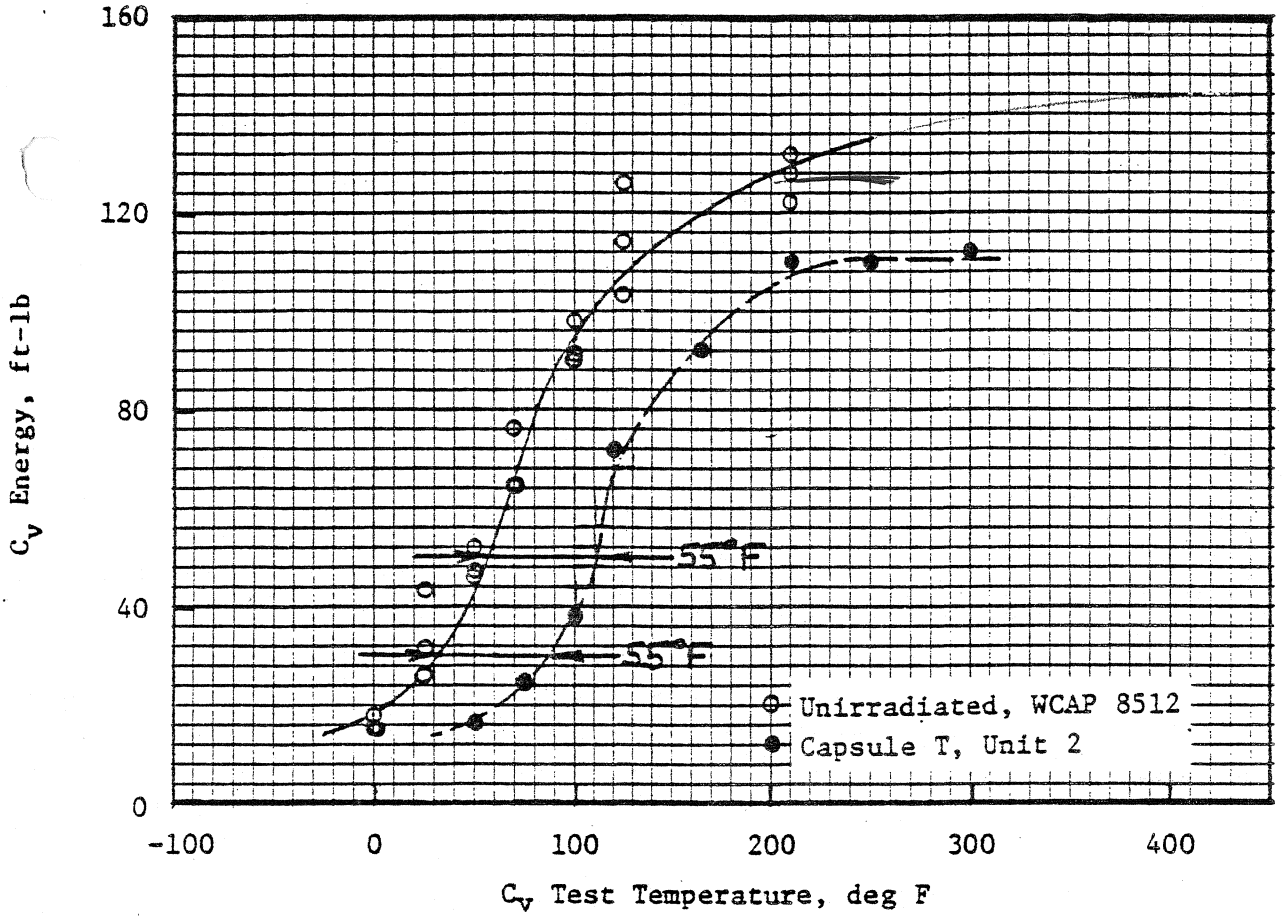

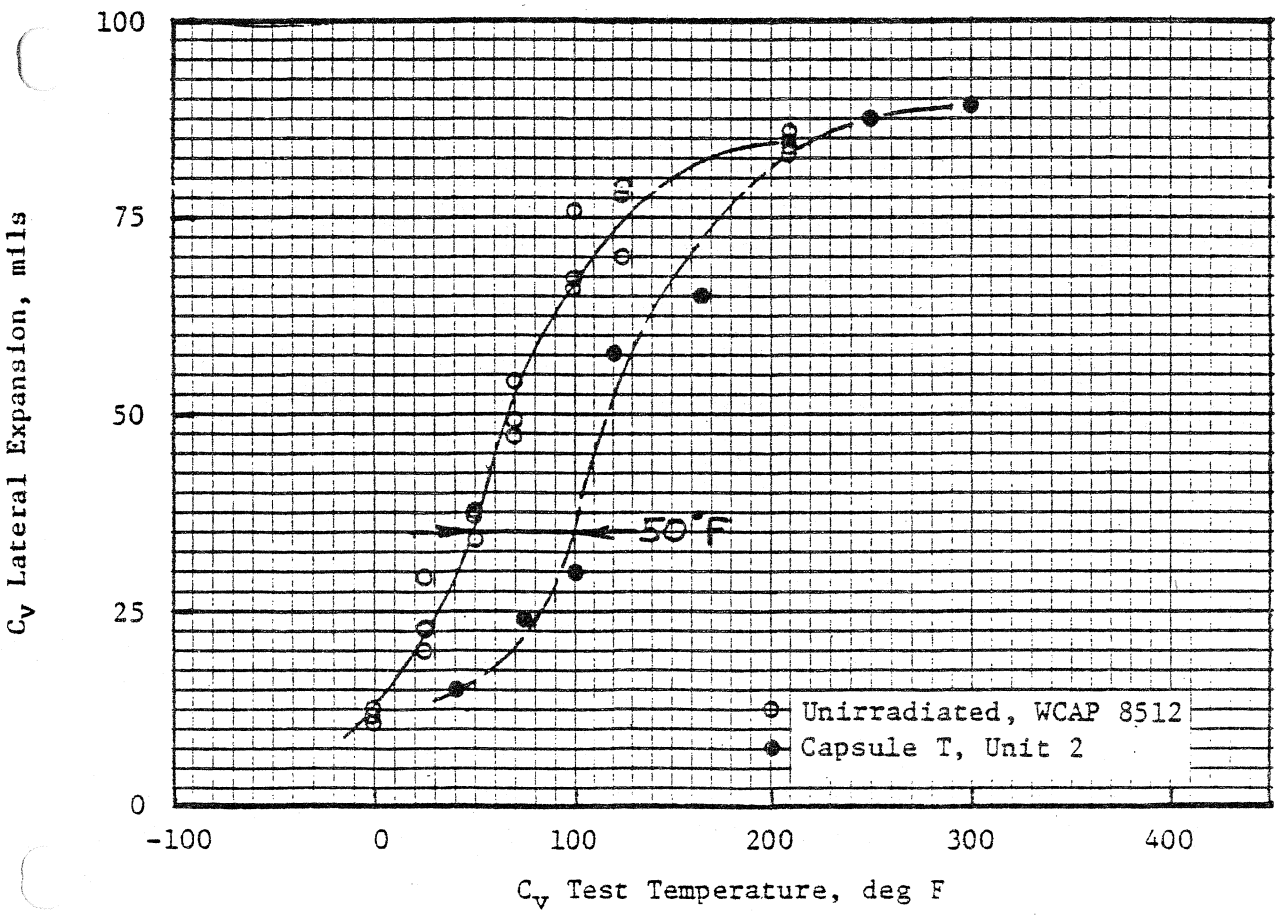

FIGURE 4. RADIATION RESPONSE OF DONALD C. COOK VESSEL SHELL PLATE C5521-2 (LONGITUDINAL ORIENTATION)

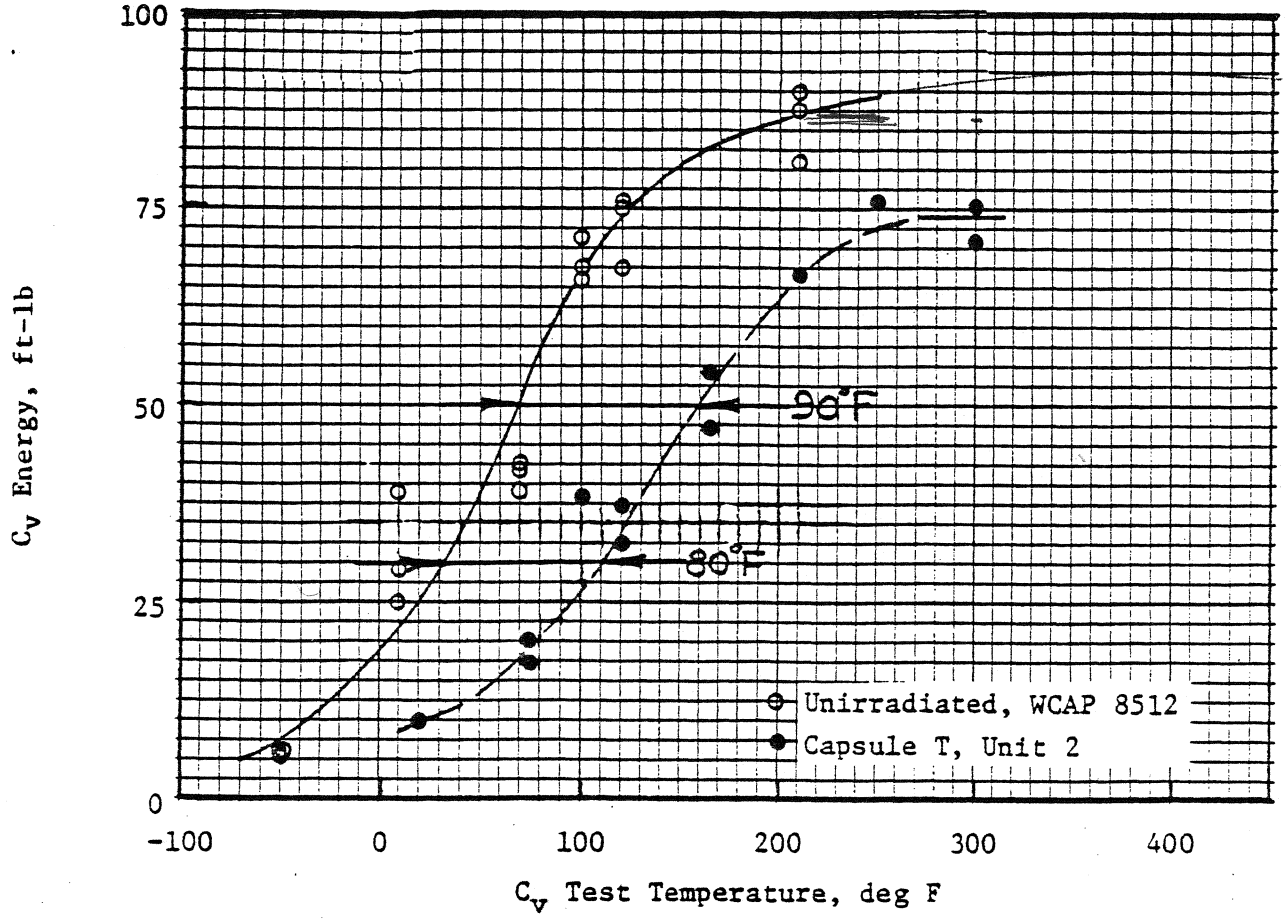

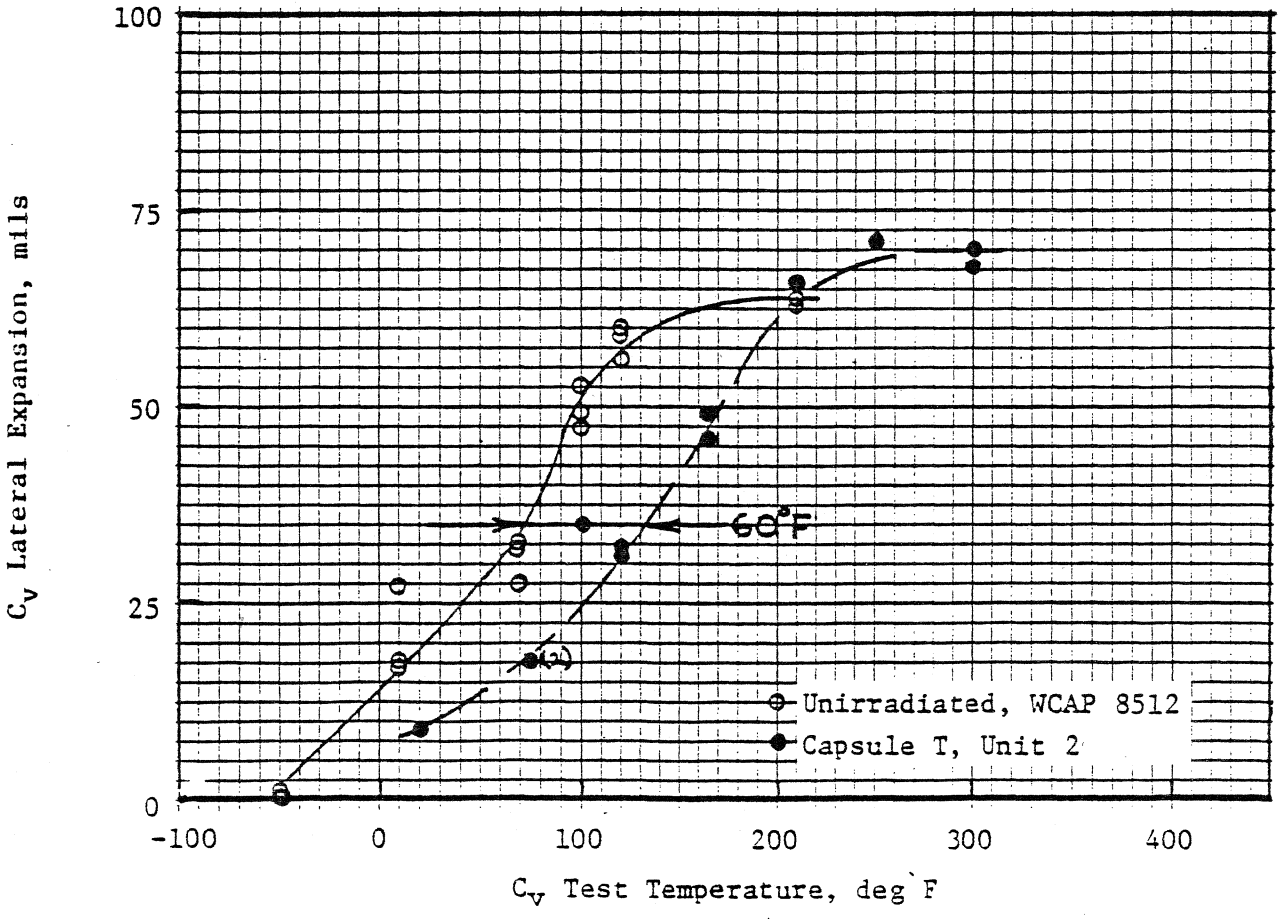

FIGURE 5. RADIATION RESPONSE OF DONALD C. COOK VESSEL SHELL PLATE C5521-2 (TRANSVERSE ORIENTATION)

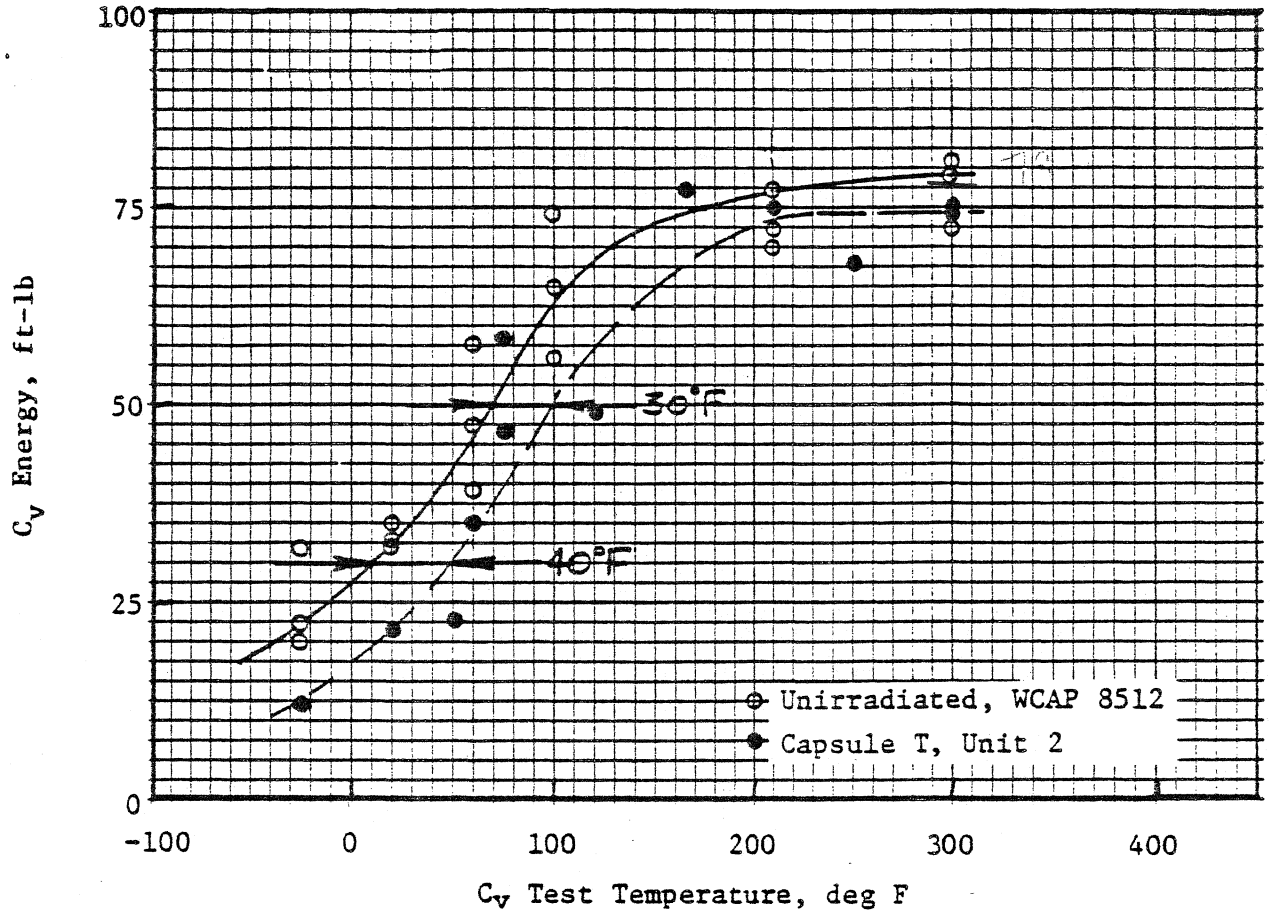

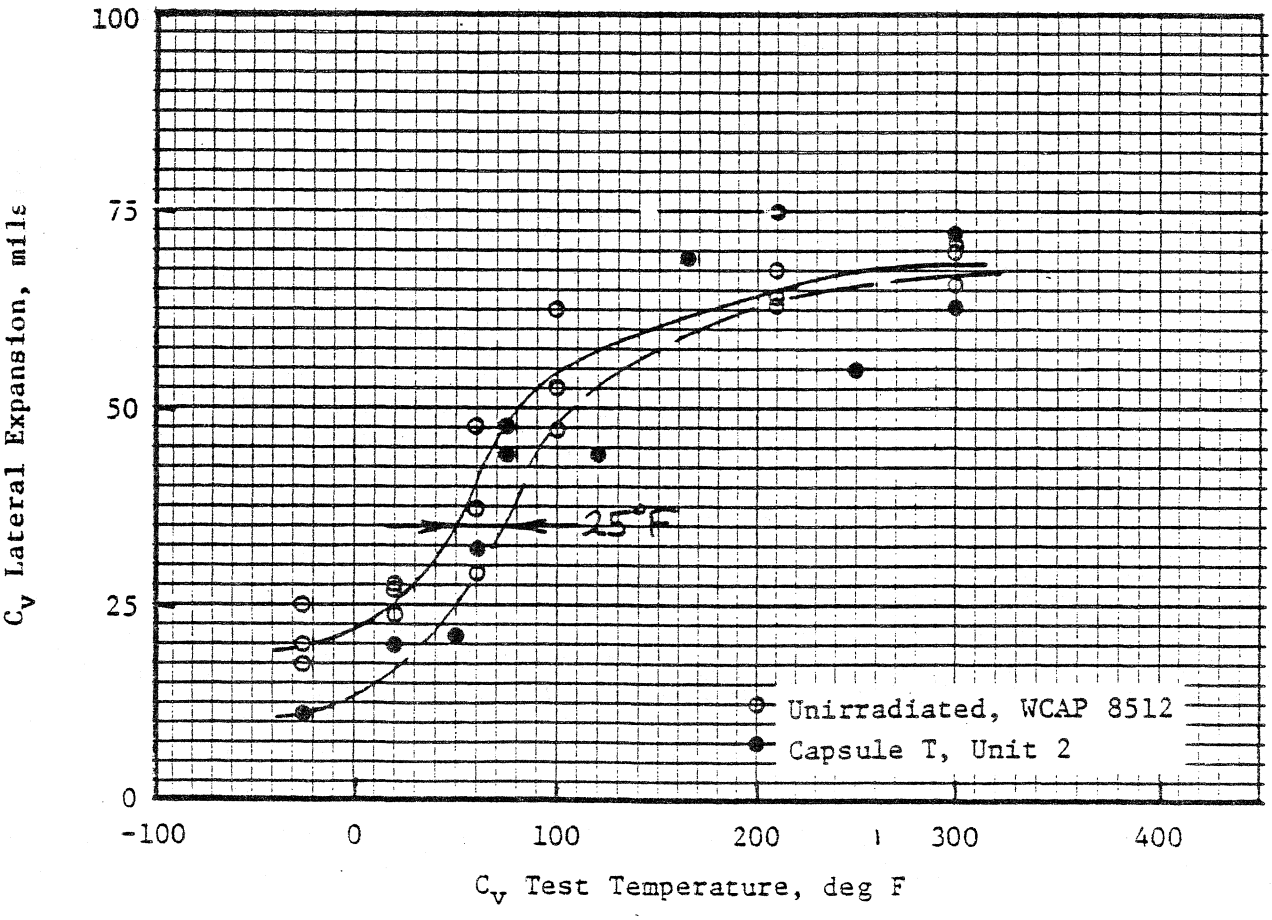

FIGURE 6. RADIATION RESPONSE OF DONALD C. COOK VESSEL CORE REGION WELD METAL

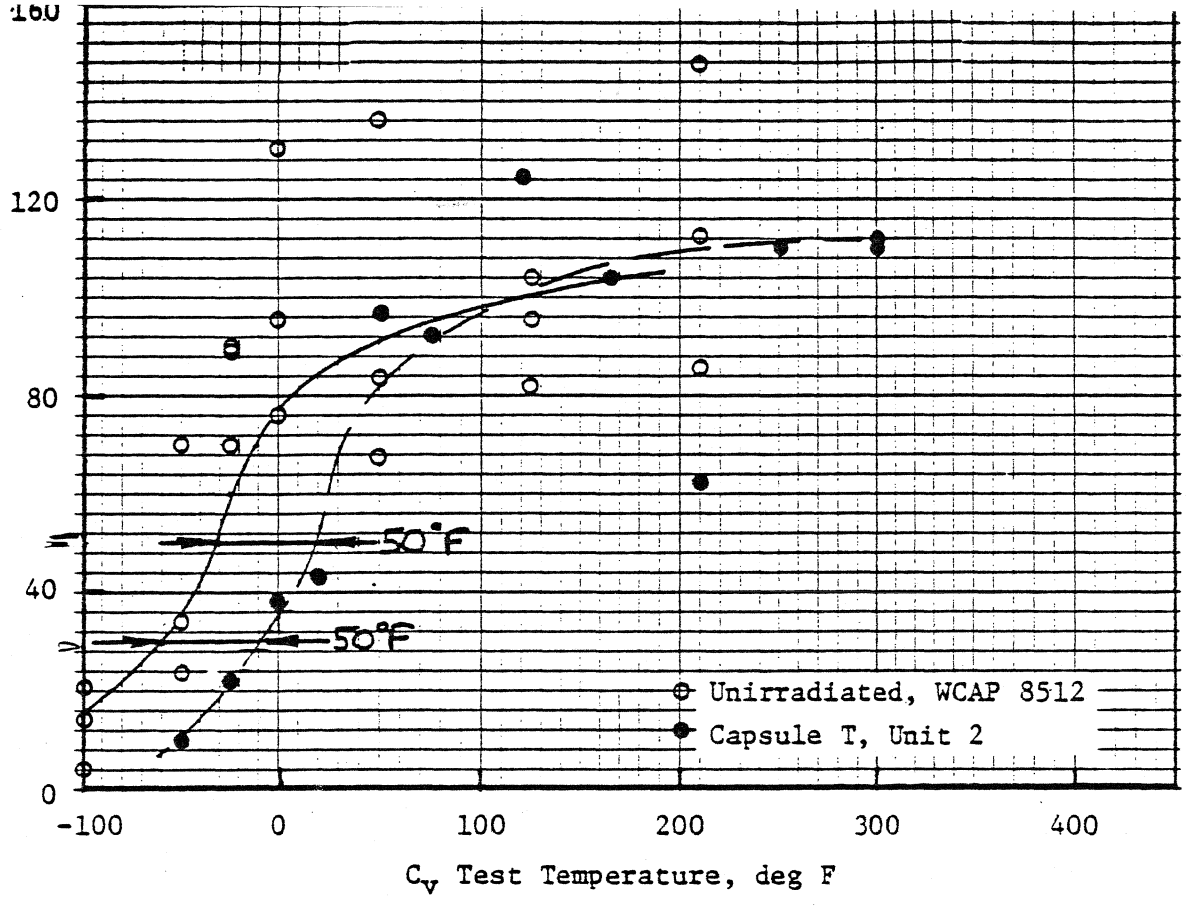

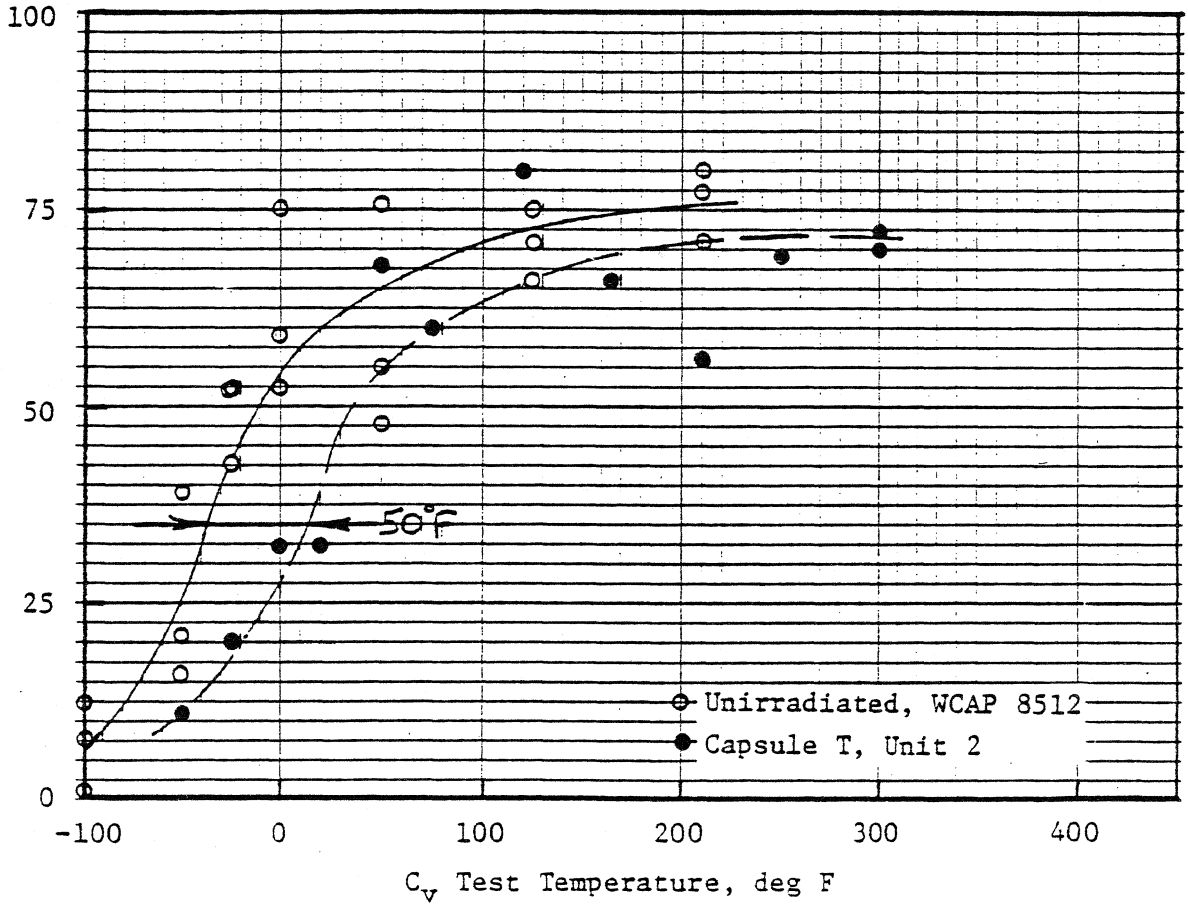

FIGURE 7. RADIATION RESPONSE OF DONALD C. COOK VESSEL CORE REGION WELD HAZ MATERIAL

TABLE IX

EFFECT OF IRRADIATION ON CAPSULE T SURVEILLANCE MATERIALS
DONALD C. COOK UNIT NO. 2

L.F. = 3.24

Criterion(1)	Weld Metal(2)	HAZ Material(2)	Trans. Plate C5521-2(3)	Long. Plate C5521-2(3)
Transition Temperature Shift	p.29	p.30	p.28	p.27
@ 50 ft-lb	30°F	50°F	90°F	55°F
@ 30 ft-lb	40°F	50°F	80°F	55°F
@ 35 mil	25°F	50°F	60°F	50°F
ΔRT_{NDT}(4)	40°F	50°F see p.26	80°F	55°F
C_V Upper Shelf Drop	2 ft-lb (3%)	22 ft-lb (18%)	12 ft-lb (14%)	16 ft-lb (12%)
UNIRR USE	78	115 (?)	90	125
Cu	0.25	110		0.11
Ni	0.11			
CF	75			91.1

(1) Refer to Figures 4-7.
(2) Fluence = 1.8×10^{18} n/cm^2, E > 1 MeV
(3) Fluence = 2.3×10^{18} n/cm^2, E > 1 Mev
(4) Maximum transition temperature shift at 30 ft-lb or 35 mil

TABLE X

TENSILE PROPERTIES OF SURVEILLANCE MATERIALS
DONALD C. COOK UNIT NO. 2

Condition	Test Material	Spec. No.	Temp. (°F)	0.2% YS (ksi)	UTS (ksi)	Fracture Load (lb)	Fracture Stress (ksi)	Uniform Elongation (%)	Total Elongation (%)	R.A. (%)
Capsule T	Plate C5521-2 (Transverse)	MT-10	250	58.7	89.9	3100	139.6	9.8	19.1	54.4
	↓	MT-9	550	66.5	88.3	3150	141.9	9.0	18.0	54.4
	Weld Metal	MW-10	210	77.0	93.7	2900	173.6	9.0	21.4	66.0
	↓	MW-9	550	67.7	90.5	3180	179.7	8.4	19.1	64.0
(a)	Plate C5521-2	-	Room	67.4	87.3	3200	161.2	13.4	23.4	59.6
	(Transverse)	-	Room	65.4	85.9	2950	156.4	15.0	27.1	61.7
	↓	-	300	58.8	78.6	2650	146.1	13.0	22.6	63.1
	↓	-	300	60.5	79.5	2675	157.6	10.6	19.8	65.4
	↓	-	550	57.5	83.0	3225	142.1	11.5	19.0	53.8
	↓	-	550	58.9	83.1	3150	145.6	12.7	20.5	56.0
	Weld Metal	-	Room	75.7	93.2	2850	173.4	13.9	25.7	66.8
	↓	-	Room	76.9	91.3	2950	178.8	12.2	22.6	66.6
	↓	-	300	70.7	88.0	2900	171.0	10.7	20.7	66.0
	↓	-	300	71.0	85.3	2875	179.0	10.3	21.2	67.5
	↓	-	550	70.0	87.2	3160	157.2	10.1	19.2	59.6
	↓	-	550	68.2	87.8	3050	166.0	9.3	20.2	62.8

dupe

(a) Unirradiated [12]

V. ANALYSIS OF RESULTS

The analysis of data obtained from surveillance program specimens has the following goals:

(1) Estimate the period of time over which the properties of the vessel beltline materials will meet the fracture toughness requirements of Appendix G of 10CFR50. This requires a projection of the measured reduction in C_v upper shelf energy to the vessel wall using knowledge of the energy and spatial distribution of the neutron flux and the dependence of C_v upper shelf energy on the neutron fluence.

(2) Develop heatup and cooldown curves to describe the operational limitations for selected periods of time. This requires a projection of the measured shift in RT_{NDT} to the vessel wall using knowledge of the dependence of the shift in RT_{NDT} on the neutron fluence and the energy and spatial distribution of the neutron flux.

The energy and spatial distribution of the neutron flux for Donald C. Cook Unit No. 2 was calculated for Capsule T with a discrete ordinates transport code. This analysis predicted that the lead factor (ratio of fast flux at the capsule location to the maximum pressure vessel flux) for Capsule T was 3.24 at the capsule centerline, 3.38 for the core-side Charpy layer, and 2.71 for the vessel-side Charpy layer (see Table III). This analysis also predicted that the fast flux at the 1/4T and 3/4T positions in the 8.5-in. pressure vessel wall would be 54% and 10%, respectively, of that at the vessel I.D. However, in this report the projection of Capsule T results to the pressure vessel wall utilizes the more conservative attenuation figures of 60% and 15% for the 1/4T and 3/4T positions to allow

for the increased fraction of neutrons which might accrue in the 0.1 to 1.0 MeV range in deep penetration situations.

A method for estimating the increase in RT_{NDT} as a function of neutron fluence and chemistry is given in Regulatory Guide 1.99, Revision 1 [8]. However, the Guide also permits the extrapolation of credible surveillance data by constructing response curves through the data points and parallel to the Guide trend curves, as shown in Figure 8.

The Donald C. Cook Unit No. 2 intermediate shell surveillance plates are projected to control the adjusted value of RT_{NDT} through the 32 EFPY design life of the pressure vessel because (1) the unirradiated values of RT_{NDT} for both intermediate shell plates are higher than those of all other reactor vessel materials [14], and (2) the intermediate shell plates are more sensitive than the other core beltline surveillance materials are to irradiation embrittlement. Intermediate shell plates C5521-2 (RT_{NDT} = 38°F, % P = 0.013, and % Cu = 0.14) and C5556-2 (RT_{NDT} = 58°F, % P = 0.014, and % Cu = 0.15) are equivalent surveillance materials in accordance with ASTM E 185-73, Annex A1 [9]. Westinghouse selected plate C5521-2 for the surveillance program because it had the lower Charpy V-notch upper shelf energy [14] as directed by Figure A1 of ASTM E 185-73. However, the vessel RT_{NDT} projections are based on an unirradiated RT_{NDT} of 58°F reported for plate C5556-2 because it is more conservative to do so. A summary of the projected values of RT_{NDT} for 12 and 32 EFPY of operation of Donald C. Cook Unit No. 2 is presented in Table VI.

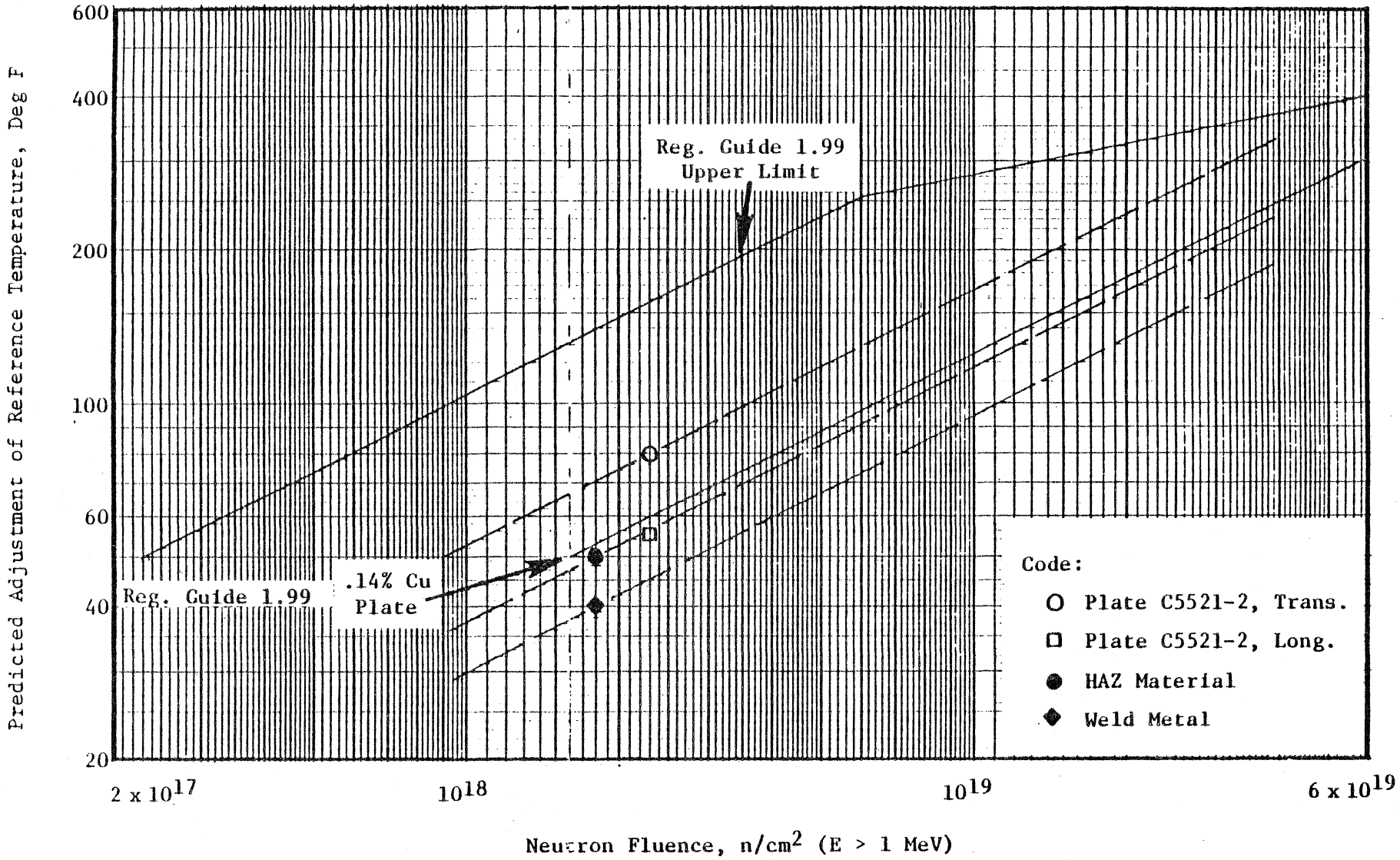

FIGURE 8. EFFECT OF NEUTRON FLUENCE ON RT_{NDT} SHIFT, DONALD C. COOK UNIT NO. 2

TABLE XI

PROJECTED VALUES OF RT_{NDT} FOR DONALD C. COOK UNIT NO. 2

EFPY	P.V. Material	Location	Initial RT_{NDT}(a)	Fluence(b)	ΔRT_{NDT}	Adj. RT_{NDT}
12	Plate ~~C5521-2~~ C5556-2 (p. 34)	I.D.	58°F	7.4×10^{18}	144	202
	↓ data used for RT_{NDT}	1/4T	58°F	4.4×10^{18}	110	168
		3/4T	58°F	1.1×10^{18}	55	113
12	HAZ Material	I.D.	20°F	7.4×10^{18}	101	121
	↓	1/4T	20°F	4.4×10^{18}	78	98
		3/4T	20°F	1.1×10^{18}	40	60
12	Weld Metal	I.D.	-35°F	7.4×10^{18}	81	46
	↓	1/4T	-35°F	4.4×10^{18}	63	28
		3/4T	-35°F	1.1×10^{18}	31	-4
32	Plate ~~C5521-2~~ C5556-2 (p. 34)	I.D.	58°F	2.0×10^{19}	235	293
	↓ data used RT_{NDT}	1/4T	58°F	1.2×10^{19}	182	240
		3/4T	58°F	3.0×10^{18}	91	149
32	HAZ Material	I.D.	20°F	2.0×10^{19}	165	185
	↓	1/4T	20°F	1.2×10^{19}	129	149
		3/4T	20°F	3.0×10^{18}	64	84
32	Weld Metal	I.D.	-35°F	2.0×10^{19}	133	98
	↓	1/4T	-35°F	1.2×10^{19}	103	68
		3/4T	-35°F	3.0×10^{18}	52	17

(a) Reference 14
(b) Neutrons/cm^2, E > 1 MeV

A method for estimating the reduction in C_v upper shelf energy as a function of neutron fluence is also given in Regulatory Guide 1.99, Revision 1 [8]. The results from Capsule T are compared to a portion of Figure 2 of Regulatory Guide 1.99, Revision 1, in Figure 9. The embrittlement responses of the pressure vessel plate and HAZ surveillance materials are in good agreement with the prediction of Regulatory Guide 1.99, Revision 1, for 0.15% Cu material. On the other hand, the shelf energy response of the weld metal is well below the corresponding design curve.

Referring to the conservative NRC design curves from Regulatory Guide 1.99 shown in Figure 9, the projected C_v shelf energies of the vessel materials are as follows:

- Plate C5521-2 (Unirradiated C_v Shelf = 86 ft-lb)

  32 EFPY at I.D. -- 62 ft-lb
  32 EFPY at 1.4T -- 64 ft-lb
  32 EFPY at 3/4T -- 70 ft-lb

- Plate C5556-2 (Unirradiated C_v Shelf = 90 ft-lb)

  32 EFPY at I.D. -- 65 ft-lb
  32 EFPY at 1/4T -- 67 ft-lb
  32 EFPY at 3/4T -- 74 ft-lb

- Weld Metal (Unirradiated C_v Shelf = 97 ft-lb)

  32 EFPY at I.D. -- 75 ft-lb
  32 EFPY at 1/4T -- 78 ft-lb
  32 EFPY at 3/4T -- 83 ft-lb

- HAZ Material (Unirradiated C_v Shelf = 109 ft-lb)

  32 EFPY at I.D. -- 78 ft-lb
  32 EFPY at 1/4T -- 82 ft-lb
  32 EFPY at 3/4T -- 89 ft-lb

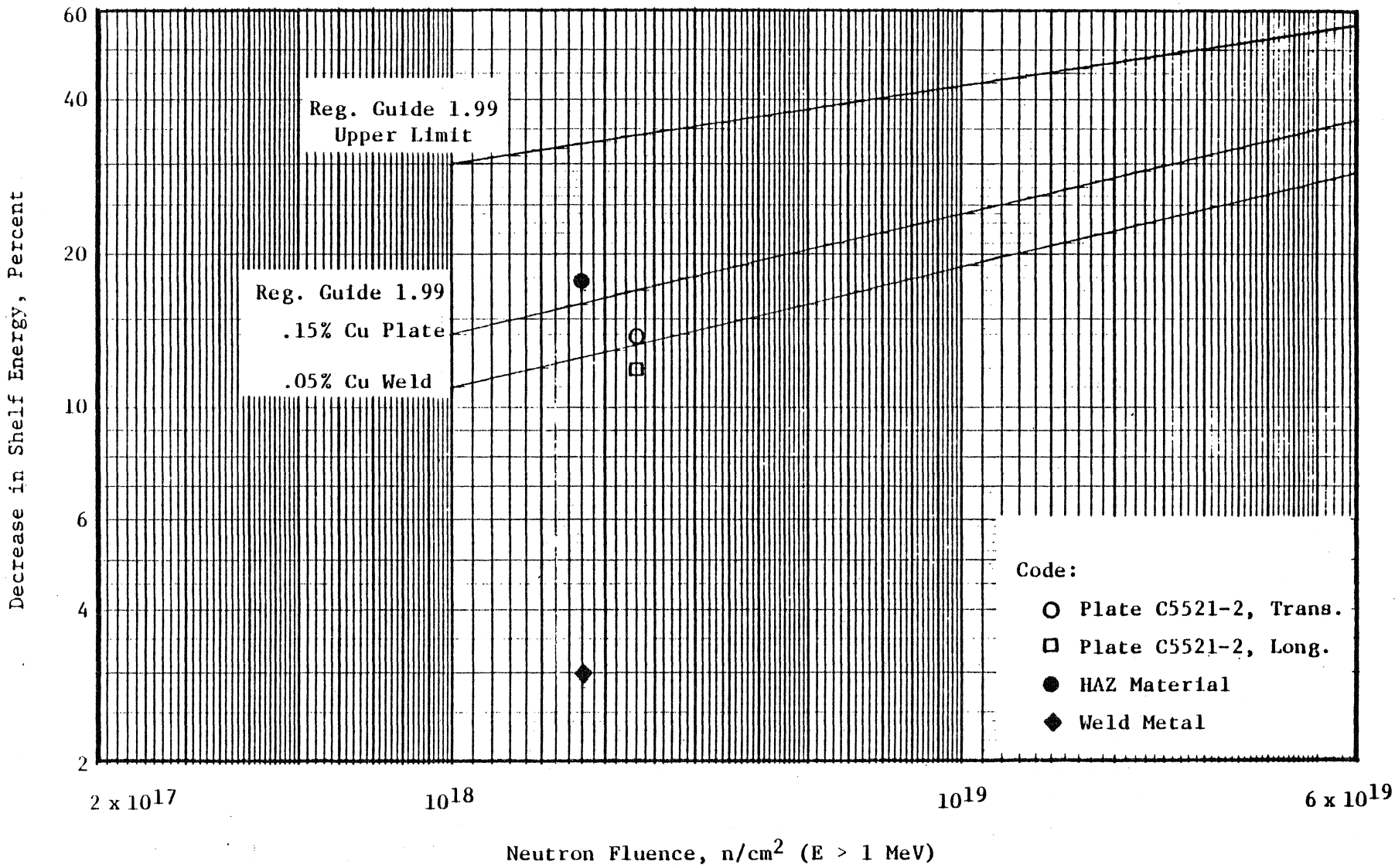

FIGURE 9. DEPENDENCE OF C_V UPPER SHELF ENERGY ON NEUTRON FLUENCE, DONALD C. COOK UNIT NO. 2

These projections indicate that the core beltline materials in the Donald C. Cook Unit No. 2 pressure vessel will retain adequate shelf toughness throughout the 32 EFPY design lifetime.

The current Donald C. Cook Unit No. 2 reactor vessel surveillance program removal schedule, revised to conform to ASTM E 185-99 [16], is summarized in Table XII. There are seven capsules remaining in the vessel, of which three are standbys.

TABLE XII

REACTOR VESSEL SURVEILLANCE CAPSULE REMOVAL SCHEDULE [14]
DONALD C. COOK UNIT NO. 2

Capsule	WOL Material	Removal Time	Equivalent Vessel Fluence
T	Weld Metal	(a)	4 EFPY at I.D.
Y	Weld Metal	3 EFPY	11 EFPY at I.D.
X	Trans. Plate	5 EFPY	E.O.L. at 1/4 T
U	Weld Metal	9 EFPY	E.O.L. at I.D.
S	Trans. Plate	32 EFPY	E.O.L. at I.D.
V	Trans. Plate	Standby	-
W	Trans. Plate	Standby	-
Z	Weld Metal	Standby	-

(a) Removed at 1.08 EFPY

VI. HEATUP AND COOLDOWN LIMIT CURVES FOR NORMAL OPERATION OF DONALD C. COOK UNIT NO. 2

Donald C. Cook Unit No. 2 is a 3391 Mw_t pressurized water reactor operated by American Electric Power Service Corporation. The unit has been provided with a reactor vessel material surveillance program as required by 10CFR50, Appendix H.

Surveillance capsule T was removed at the first refueling during the 1979 outage. This capsule was tested as described in earlier sections of this report. In summary, these test results indicate that:

(1) The RT_{NDT} of the surveillance materials in Capsule T increased a maximum of 80°F as a result of exposure to a neutron fluence of 2.2×10^{18} neutrons/cm^2 (E > 1 MeV).

(2) Based on a ratio of 3.24 between the fast neutron flux at the radial center of Capsule T and the maximum incident on the vessel wall, the vessel wall fluence at the I.D. was 6.7×10^{17} neutrons/cm^2 (E > 1 MeV) at the time of removal of Capsule T.

(3) The maximum shift in RT_{NDT} after 12 effective full power years (EFPY) of operation was predicted to be 168°F at the 1/4T and 113°F at the 3/4T vessel wall locations, as controlled by the intermediate shell plate material.

(4) The maximum shift in RT_{NDT} after 32 EFPY of operation was predicted to be 240°F at the 1/4T and 149°F at the 3/4T vessel wall locations, as controlled by the intermediate shell plate material.

The Unit No. 2 heatup and cooldown limit curves for 12 EFPY and 32 EFPY have been computed on the bases of (3) and (4) above. The procedures employed by SwRI are described in Appendix B.

The following pressure vessel constants were employed as input data in this analysis:

Vessel Inner Radius, r_i	=	86.50 in., including cladding
Vessel Outer Radius, r_o	=	95.2 in.
Operating Pressure, P_o	=	2235 psig
Initial Temperature, T_o	=	70°F
Final Temperature, T_f	=	550°F
Effective Coolant Flow Rate, Q	=	134.6 x 10^6 lb_m/hr
Effective Flow Area, A	=	26.72 ft^2
Effective Hydraulic Diameter, D	=	15.05 in.

Heatup curves were computed for a heatup rate of 100°F/hr. Since lower rates tend to raise the curve in the central region (see Appendix B), these curves apply to all heating rates up to 60°F/hr. Cooldown curves were computed for cooldown rates of 0°F/hr (steady state), 20°F/hr, 40°F/hr, 60°F/hr, and 100°F/hr. The 20°F/hr curve would apply to cooldown rates up to 20°F/hr; the 40°F/hr curve would apply to rates up to 40°F/hr; the 60°F/hr curve would apply to rates up to 60°F/hr; the 100°F/hr curve would apply to rates up to 100°F/hr.

The Unit No. 2 heatup and cooldown curves for up to 12 EFPY are given in Figures 10 and 11; those for up to 32 EFPY are given in Figures 12 and 13.

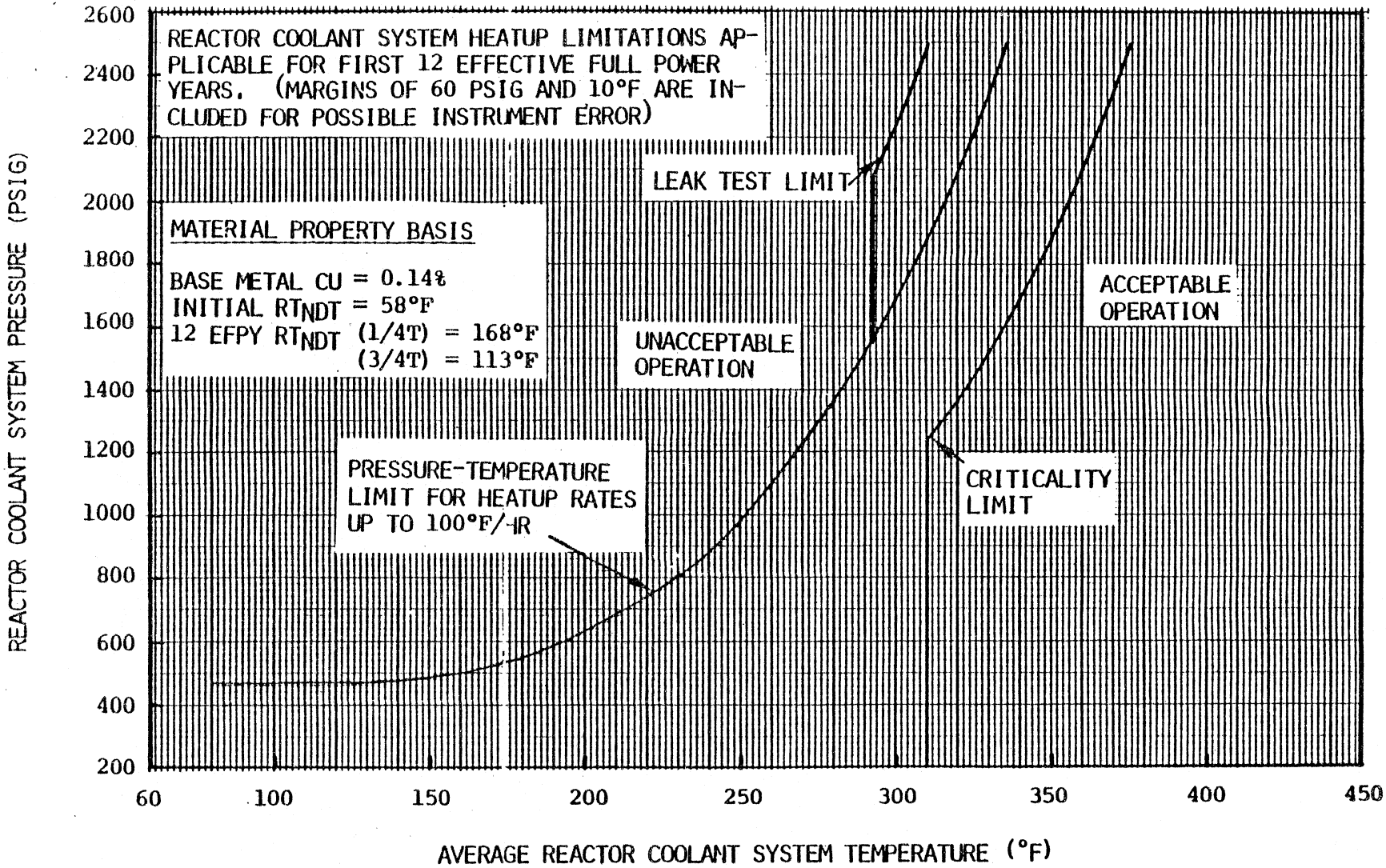

FIGURE 10. REACTOR COOLANT SYSTEM PRESSURE-TEMPERATURE LIMITS VERSUS 100°F/HOUR RATE CRITICALITY LIMIT AND HYDROSTATIC TEST LIMIT, 12 EFPY

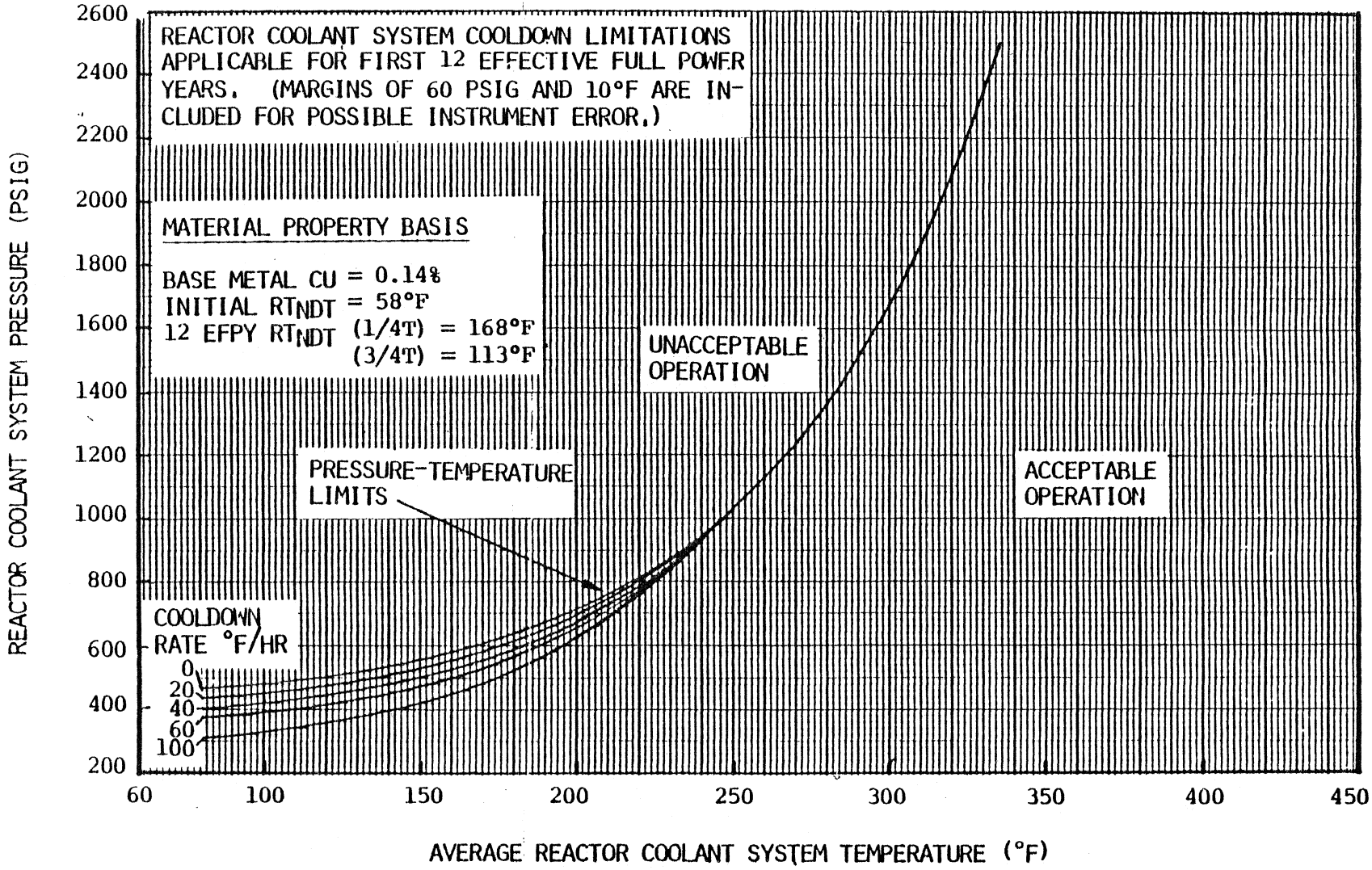

FIGURE 11. REACTOR COOLANT SYSTEM PRESSURE-TEMPERATURE LIMITS VERSUS COOLDOWN RATES, 12 EFPY

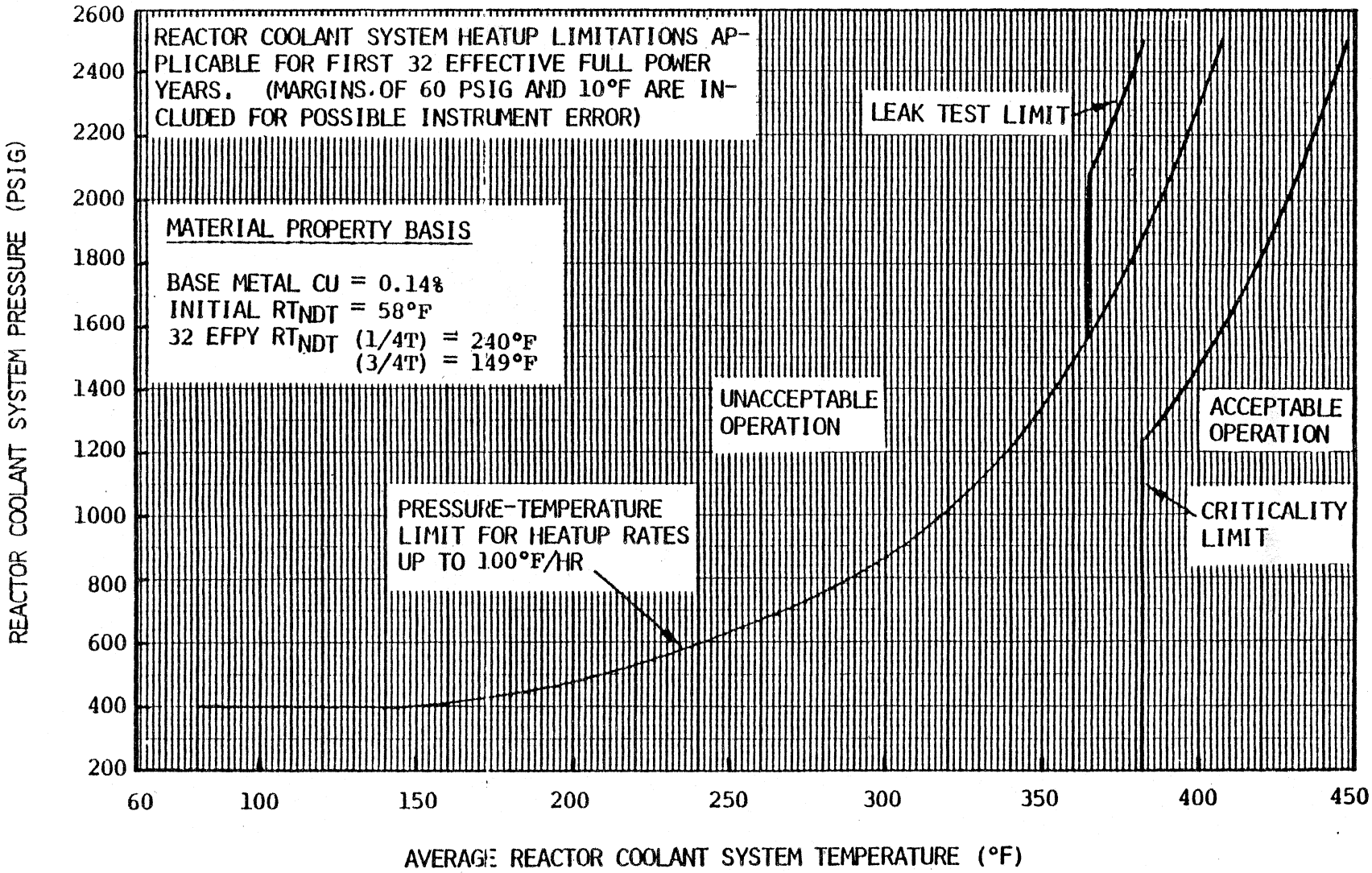

FIGURE 12. REACTOR COOLANT SYSTEM PRESSURE-TEMPERATURE LIMITS VERSUS 100°F/HOUR RATE CRITICALITY LIMIT AND HYDROSTATIC TEST LIMIT, 32 EFPY

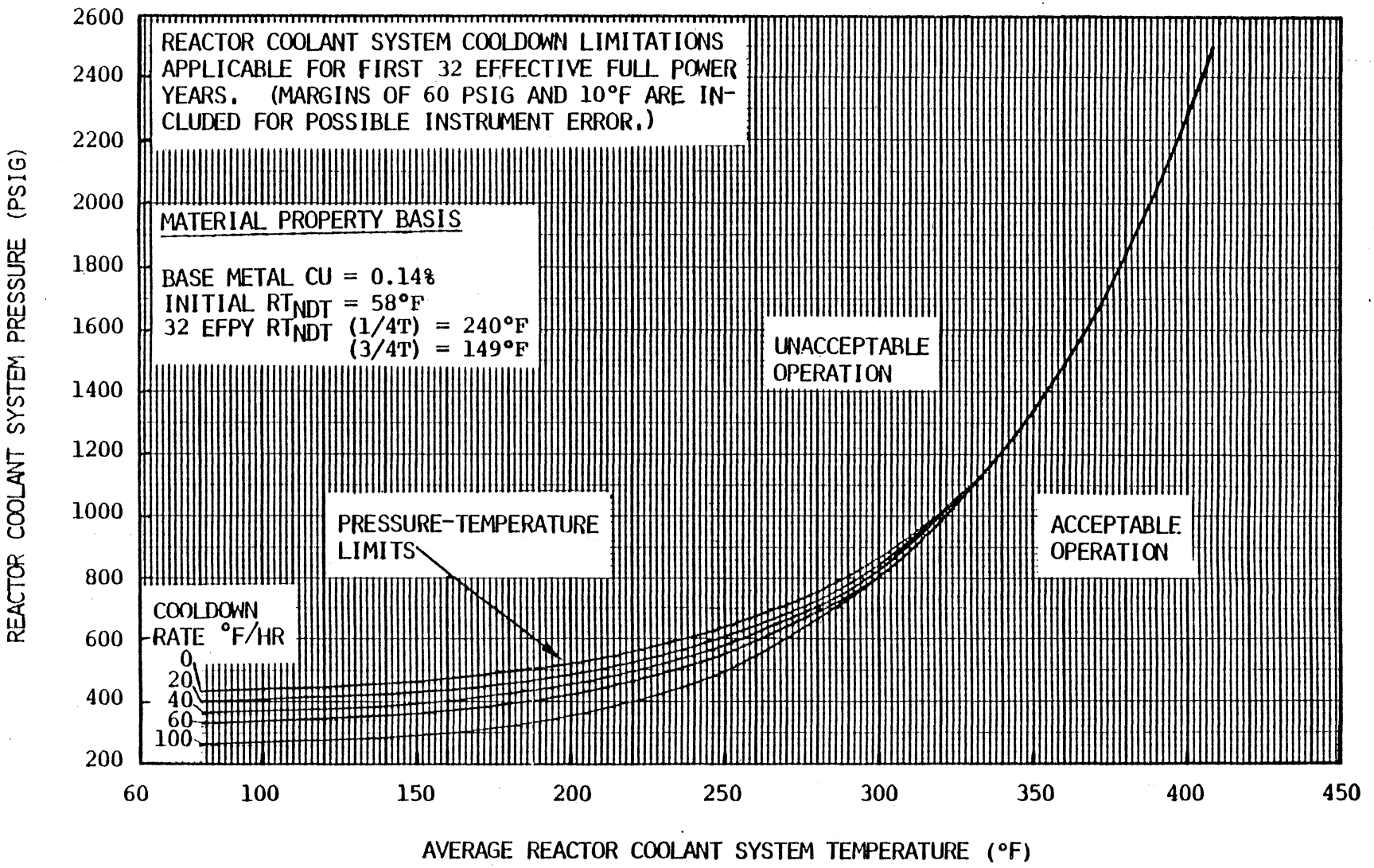

FIGURE 13. REACTOR COOLANT SYSTEM PRESSURE-TEMPERATURE LIMITS VERSUS COOLDOWN RATES, 32 EFPY

VII. REFERENCES

1. Title 10, Code of Federal Regulations, Part 50, "Licensing of Production and Utilization Facilities."

2. ASME Boiler and Pressure Vessel Code, Section III, "Nuclear Power Plant Components," 1974 Edition.

3. ASTM E 208-69, "Standard Method for Conducting Drop-Weight Test to Determine Nil-Ductility Transition Temperature of Ferritic Steels," 1975 Annual Book of ASTM Standards.

4. Steele, L. E., and Serpan, C. Z., Jr., "Analysis of Reactor Vessel Radiation Effects Surveillance Programs," ASTM STP 481, December 1970.

5. Steele, L. E., "Neutron Irradiation Embrittlement of Reactor Pressure Vessel Steels," International Atomic Energy Agency, Technical Reports Series No. 163, 1975.

6. ASME Boiler and Pressure Vessel Code, Section XI, "Rules for Inservice Inspection of Nuclear Power Plant Components," 1974 Edition.

7. "Prediction of Shift in the Ductile-Brittle Transition Temperature of LWR Pressure Vessel Materials," prepared by the Metal Properties Council, Subcommittee 6 on Nuclear Materials, July 1, 1980.

8. Regulatory Guide 1.99, Revision 1, Office of Standards Development, U. S. Nuclear Regulatory Commission. April 1977.

9. ASTM E 185-73, "Standard Recommended Practice for Surveillance Tests for Nuclear Reactor Vessels," 1975 Annual Book of ASTM Standards.

10. ASTM E 399-74, "Standard Method to Test for Plane-Strain Fracture Toughness of Metallic Materials," 1975 Annual Book of ASTM Standards.

11. Witt, F. J. and Mager, T. R., "A Procedure for Determining Bounding Values of Fracture Toughness K_{Ic} at Any Temperature," ORNL-TM-3894, October 1972.

12. "Donald C. Cook Unit No. 2 Reactor Vessel Radiation Surveillance Program," WCAP-8512, November 1975.

ADDENDUM TO FINAL REPORT

ON

"REACTOR VESSEL MATERIAL SURVEILLANCE PROGRAM FOR DONALD C. COOK UNIT NO. 2, ANALYSIS OF CAPSULE T"

Add the following references as page 48:

13. Letter, F. Noon of Westinghouse to J. R. Jensen of the American Electric Power Service Corporation, Document AEP-80-528, March 19, 1980.

14. Donald C. Cook Unit No. 2 Technical Specifications.

15. US NRC Standard Review Plan, NUREG-75/087, Section 5.3.2, Pressure-Temperature Limits, November 24, 1975.

16. ASTM E 185-79, "Standard Practice for Conducting Surveillance Tests for Light-Water Cooled Nuclear Power Reactor Vessels," 1979 Annual Book of ASTM Standards.

Approved in General
JRJ 6/7/82

APPENDIX A

TENSILE TEST RECORDS

Southwest Research Institute
Department of Materials Sciences

TENSILE TEST DATA SHEET

Test No. T- 1 | Est. U.T.S. _____ psi | Project No. 02-5928-001

Spec. No. MW-10 | Initial G.L. 1.0 in. | Machine No. 50K

Temperature +210 °F | Initial Dia. .250 in. | Date 5-2-80

Strain Rate _____ | Initial Thickness _____ in. | Initial Area .0491

Initial Width _____ in.

Top Temperature _____ °F | Maximum Load 4600 lb

Bottom Temperature _____ °F | 0.2% Offset Load 3780 lb

Final Gage Length 1.214 in. | 0.02% Offset Load _____ lb

Final Diameter .146 in. | Upper Yield Point _____ lb

Final Area .0167 in.^{2}

$$\text{U.T.S.} = \frac{\text{Maximum Load}}{\text{Initial Area}} = 93.7 \text{ KSI}$$

$$\text{0.2\% Y.S.} = \frac{\text{0.2\% Offset Load}}{\text{Initial Area}} = 77.0 \text{ KSI}$$

$$\text{0.02\% Y.S.} = \frac{\text{0.02\% Offset Load}}{\text{Initial Area}} = \_\_\_\_\_ \text{ psi}$$

$$\text{Upper Y.S.} = \frac{\text{Upper Yield Point}}{\text{Initial Area}} = \_\_\_\_\_ \text{ psi}$$

$$\text{\% Elongation} = \frac{\text{Final G.L.} - \text{Initial G.L.}}{\text{Initial G.L.}} \times 100 = 21.4\%$$

$$\text{\% R.A.} = \frac{\text{Initial Area} - \text{Final Area}}{\text{Initial Area}} \times 100 = 66.0\%$$

Signature: _____

Retrieved Test Harry E Clarke Jr 2 May 80

Spec # MW-10
May 2, 1980

Load/Strain Record

See Cal Sheet may 2, 1980 for detail

$\dot{X}$ = .006 inch/minute

TEST TEMP 210° F

$P_y = (6.0")(1K/in) = 6.0K$

$\sigma_y = \frac{6.0K}{.049"} = 122.2Ksi$

$\epsilon_y = 10 \times 10^{-3}$ ~~4.0e-3~~

E = 30.5 msi

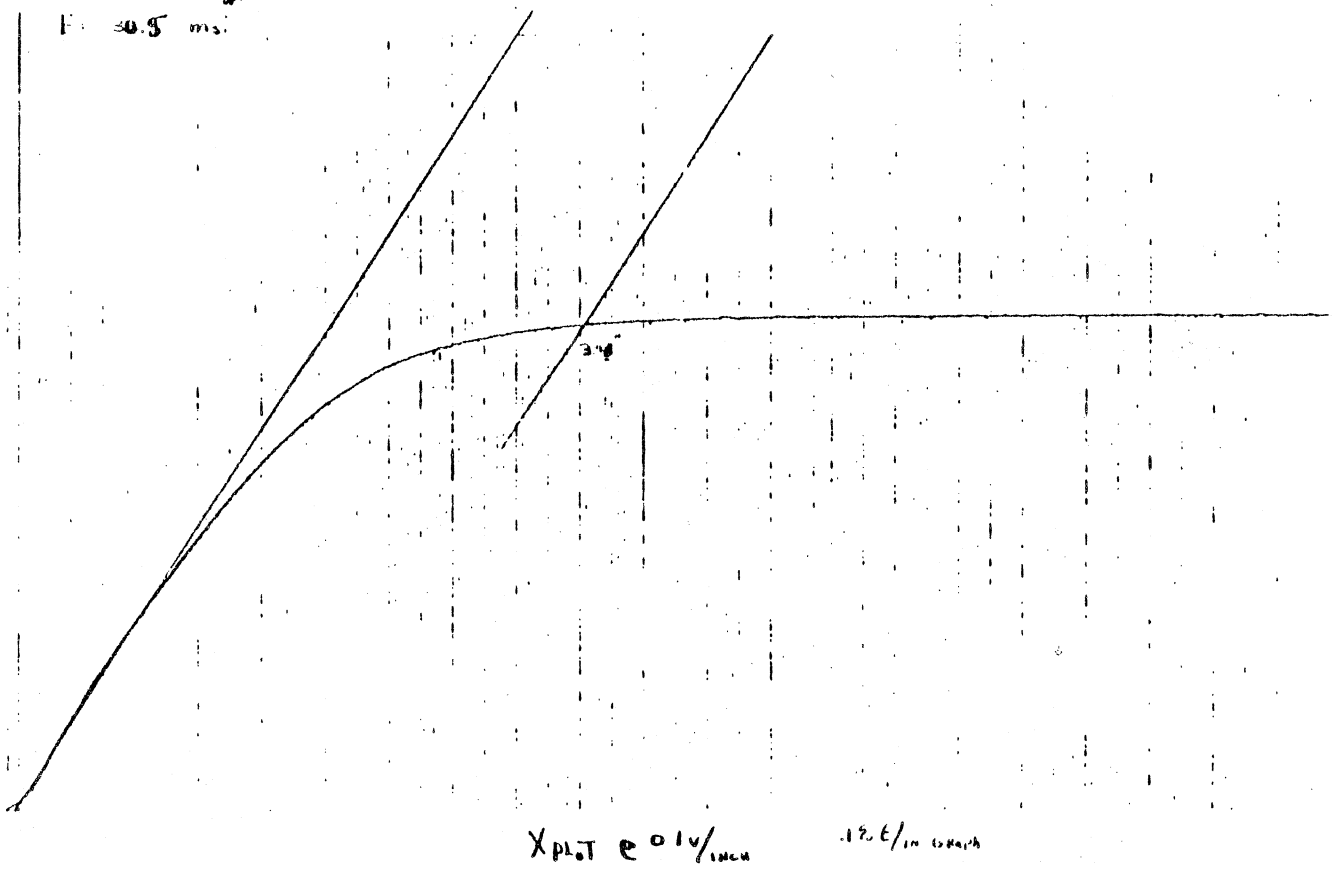

P_{max} = 4.6 Kip

P_y = 3.77 Kip

4.6"

$\sigma_{UTS} = \frac{(4.6")(1K/in)}{.049in^2} = 93.9Ksi$

$\sigma_{ys} = \frac{(3.77")(1K/in)}{.049in^2} = 77.0Ksi$

Y plot @ 1.0 v/inch

X plot @ 0.1 v/inch .1% ε/in (Strain)

Spec # MIL-10

May 2, 1980

Load/Displacement Record

See Cal. Sheet may 2, 1980 for data

Begin $\dot{X}$ @ .006 inch/minute

TEST TEMP 210°F

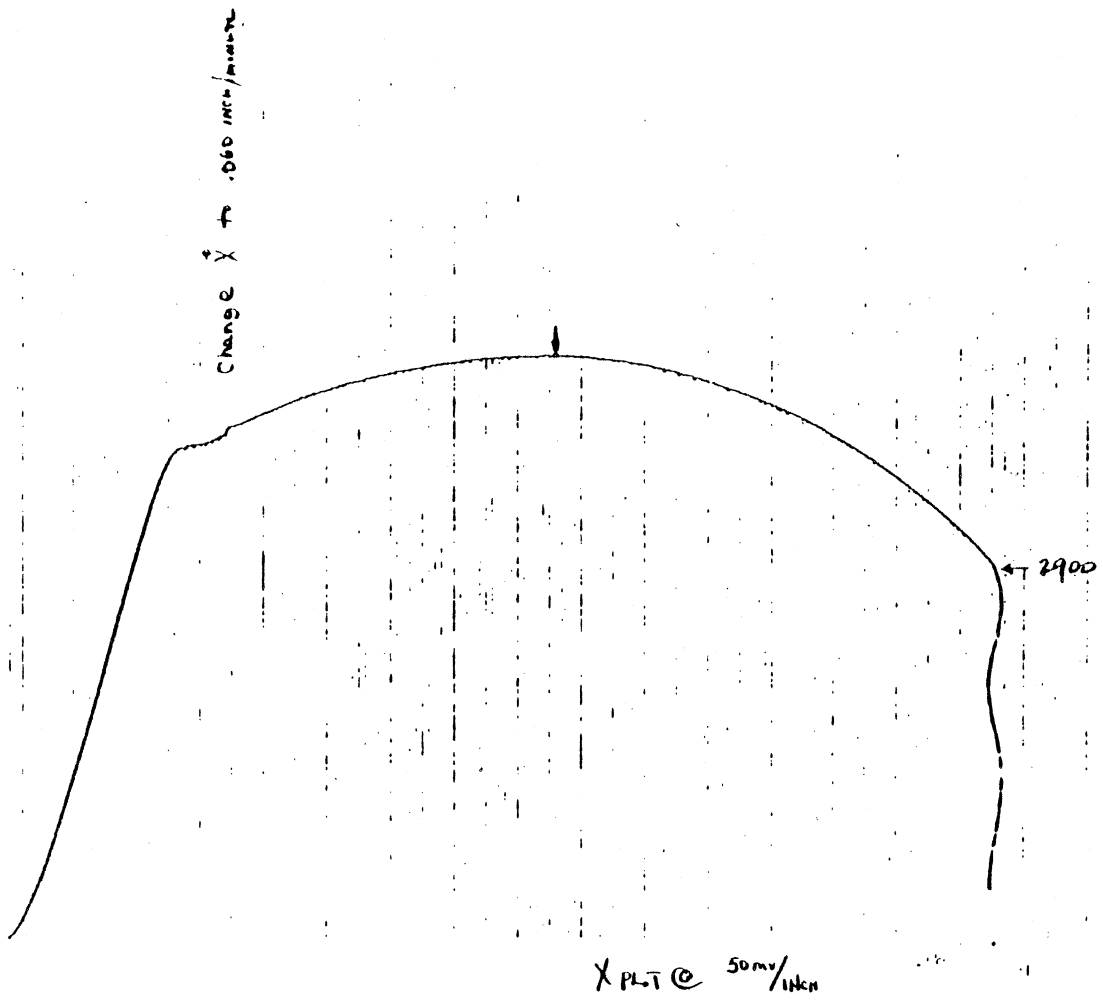

Southwest Research Institute
Department of Materials Sciences

TENSILE TEST DATA SHEET

Test No. T-_____ Est. U.T.S. _____ psi Project No. 02-5928-001

Spec. No. MW-9 Initial G.L. 1.0 in. Machine No. 50K

Temperature +550 °F Initial Dia. .250 in. Date 5-21-80

Strain Rate _____ Initial Thickness _____ in. Initial Area .0491 in^2 (DV)

Initial Width _____ in.

Top Temperature 554 °F Maximum Load 4445 (DV) lb

Bottom Temperature 551 °F 0.2% Offset Load 3325 (DV) lb

Final Gage Length 1.191 in. 0.02% Offset Load _____ (DV) lb

Final Diameter .150 in. Upper Yield Point _____ lb

Final Area .0177 (DV) in.^{2}

$$\text{U.T.S.} = \frac{\text{Maximum Load}}{\text{Initial Area}} = \frac{90.5}{\text{(DV)}} \text{ ~~psi~~ Ksi}$$

$$\text{0.2\% Y.S.} = \frac{\text{0.2\% Offset Load}}{\text{Initial Area}} = \frac{67.7}{\text{(DV)}} \text{ ~~psi~~ Ksi}$$

$$\text{0.02\% Y.S.} = \frac{\text{0.02\% Offset Load}}{\text{Initial Area}} = \_\_\_\_\_ \text{ psi}$$

$$\text{Upper Y.S.} = \frac{\text{Upper Yield Point}}{\text{Initial Area}} = \_\_\_\_\_ \text{ psi}$$

$$\text{\% Elongation} = \frac{\text{Final G.L.} - \text{Initial G.L.}}{\text{Initial G.L.}} \times 100 = \frac{19.1}{\text{(DV)}} \text{ \%}$$

$$\text{\% R.A.} = \frac{\text{Initial Area} - \text{Final Area}}{\text{Initial Area}} \times 100 = \frac{64.0}{\text{~~63.4~~ (DV)}} \text{ \%}$$

Tested by: R. Ayers

Spec # MW-4
May 21, 1980
Load/Strain
$\dot{\lambda}$ = .006 IN/min
Temp + 550°F
02-5928-001

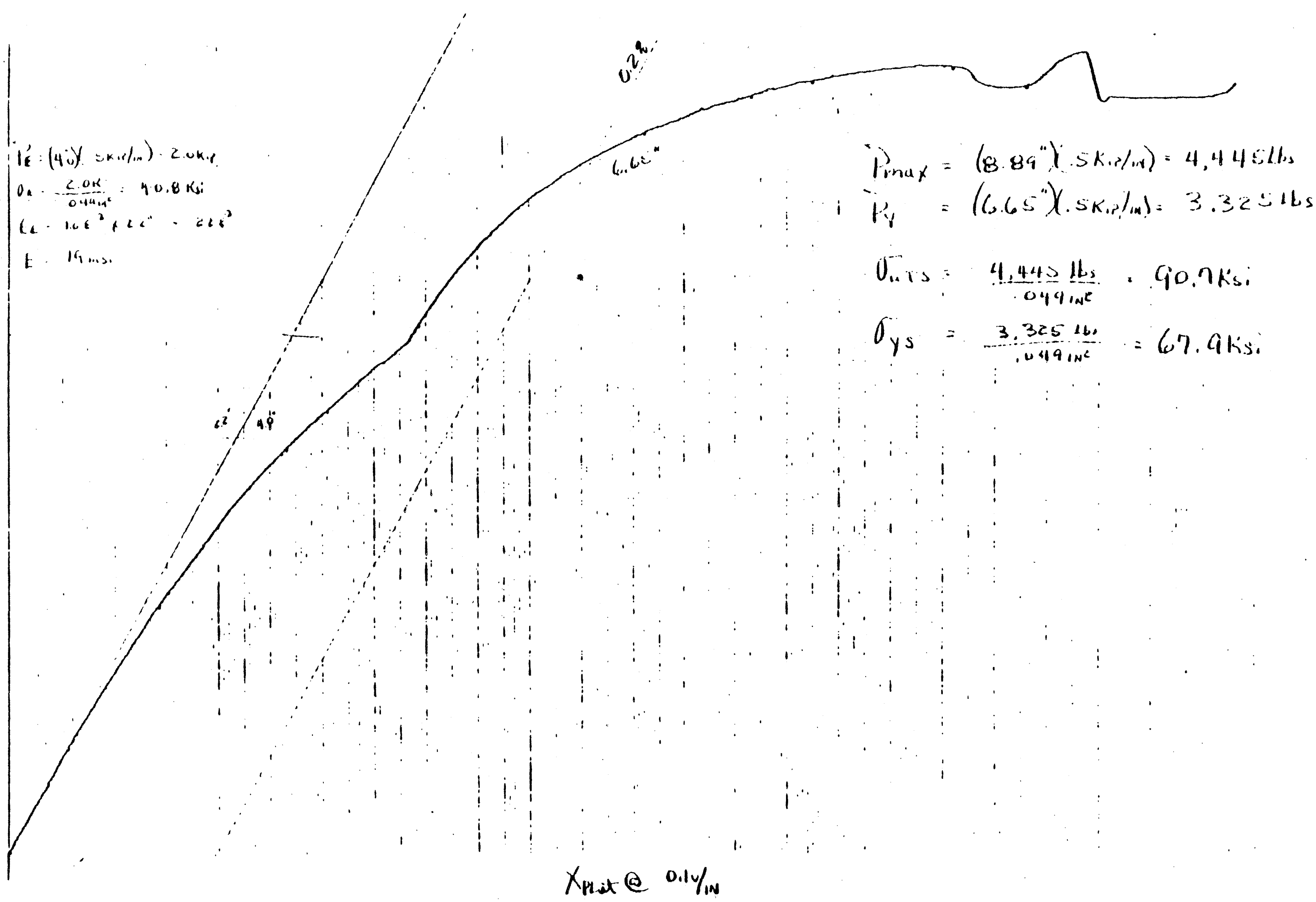

Spec #MW-9

May 21, 402
Load/Displacement
$\dot{\varepsilon}$ = .006 IN/min
Temp is 550°F
02-5928-001

P_{max} = (8.89")( ) = 4445 lbs

elongation @ P_{max} = (2.65")(.0322) = .0853 inches

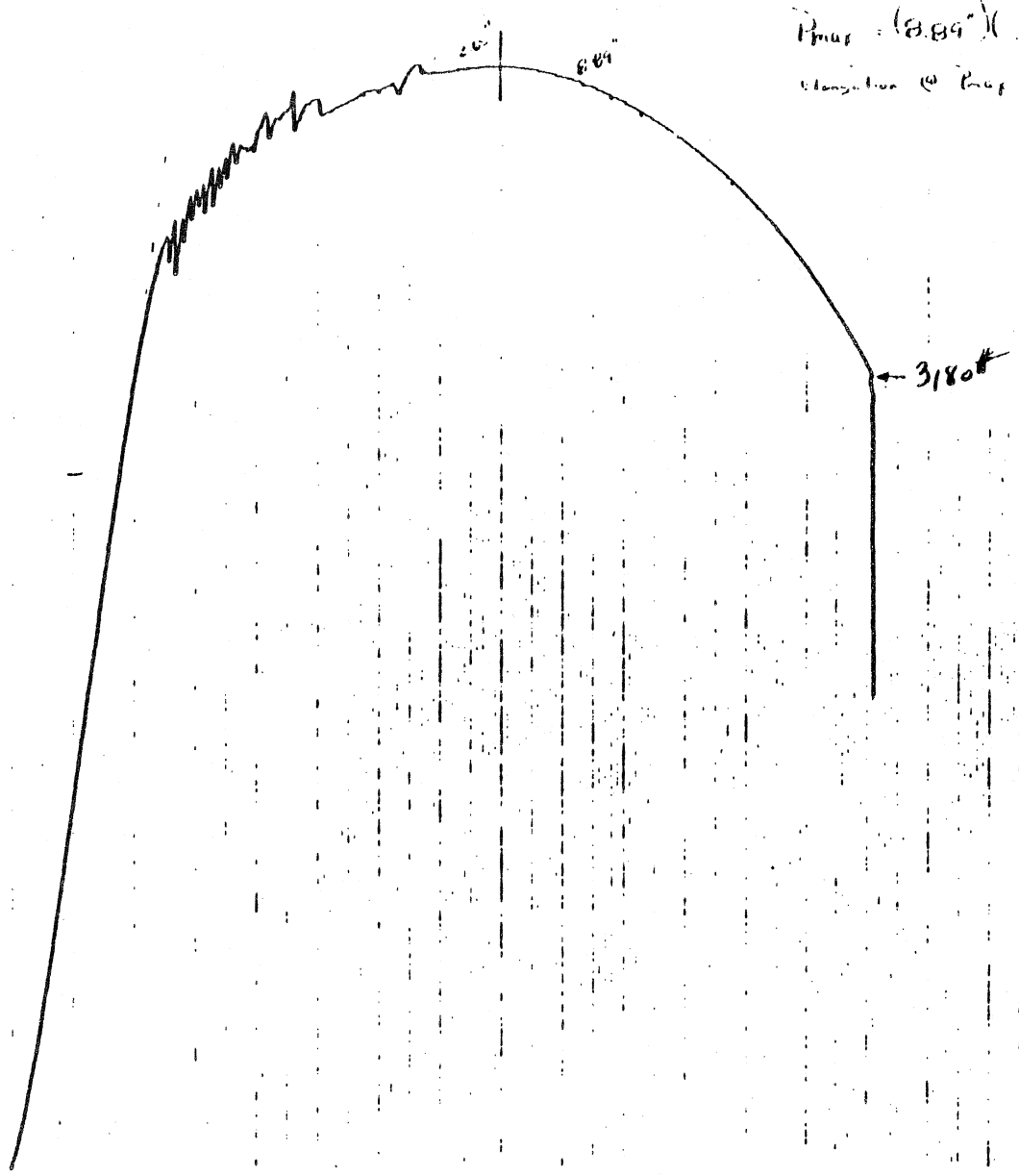

Xplot @ 50mV/in

Yplot @ 0.5V/in

Southwest Research Institute
Department of Materials Sciences

TENSILE TEST DATA SHEET

Test No. T- 2 | Est. U.T.S. _____ psi | Project No. 02-5522-001

Spec. No. MIL-10 | Initial G.L. 1.0 in. | Machine No. 50K

Temperature +250°F | Initial Dia. .249 in. | Date 5-2-80

Strain Rate _____ | Initial Thickness _____ in. | Initial Area .0487 (60)

Initial Width _____ in.

Top Temperature _____ °F | Maximum Load 4,389 (60) lb

Bottom Temperature _____ °F | 0.2% Offset Load 2,839 (60) lb

Final Gage Length 1.191 in. | 0.02% Offset Load _____ lb

Final Diameter .168 in. | Upper Yield Point _____ lb

Final Area .0222 (60) in.^{2}

$$\text{U.T.S.} = \frac{\text{Maximum Load}}{\text{Initial Area}} = \frac{89.9 \text{ (60)}}{} \text{ KSI}$$

$$\text{0.2\% Y.S.} = \frac{\text{0.2\% Offset Load}}{\text{Initial Area}} = \frac{58.7 \text{ (60)}}{} \text{ KSI}$$

$$\text{0.02\% Y.S.} = \frac{\text{0.02\% Offset Load}}{\text{Initial Area}} = \_\_\_\_\_ \text{ psi}$$

$$\text{Upper Y.S.} = \frac{\text{Upper Yield Point}}{\text{Initial Area}} = \_\_\_\_\_ \text{ psi}$$

$$\text{\% Elongation} = \frac{\text{Final G.L.} - \text{Initial G.L.}}{\text{Initial G.L.}} \times 100 = \frac{19.1 \text{ (60)}}{} \%$$

$$\text{\% R.A.} = \frac{\text{Initial Area} - \text{Final Area}}{\text{Initial Area}} \times 100 = \frac{54.4 \text{ (60)}}{} \%$$

Signature: [signature]

Witnessed Test Harry R Clark Jr RE QA 2 May 80

May 2, 1980

Load/strain record

See Cal. Sheet May 2, 1980 for data

$\dot{X}$ = .006 inch/minute

TEST TEMP 260°F

P_{ys} (0.2) (1K/in) = 6.0K

σ_{ys} = 6.0 / .0489 in² = 123.2 Ksi

ϵ_{ys} = 1.0 e-3 (4.00 4.90 e-3)

E = 29.3 (~~30.3~~) msi

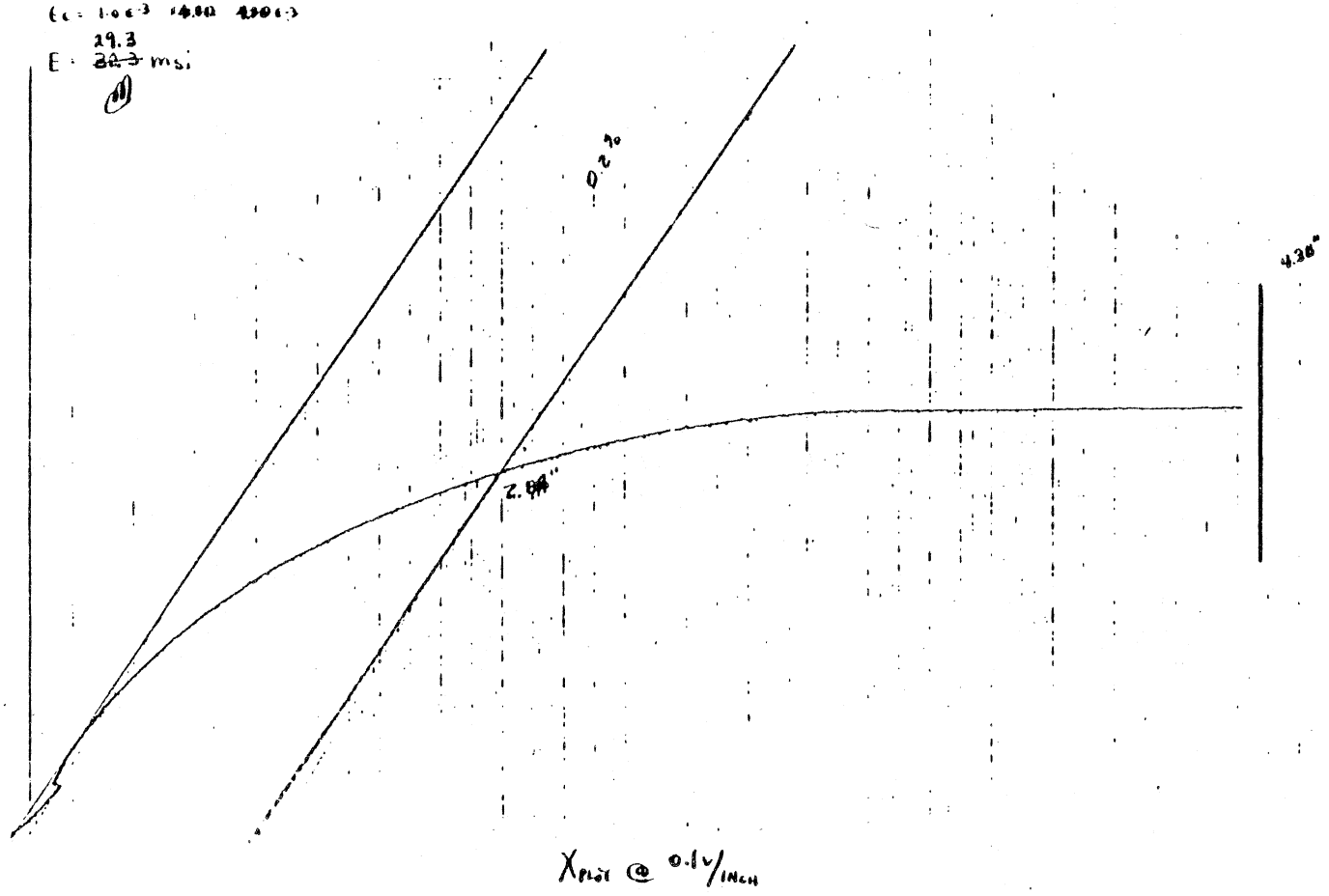

Y_{plot} @ 1.0 v/inch

X_{plot} @ 0.1 v/inch

P_{max} = 4.38 K/#

P_y = 2.83 K/#

$\sigma_{UTS} = \frac{(4.38)(1K/in)}{.0489\ in^2} = 89.4$ Ksi

$\sigma_{ys} = \frac{(2.84)(1K/in)}{.0489\ in^2} = 58.1$ Ksi

Spec # MT-10

May 2, 1980

Load/Displacement Record

See Cal. Sheet May 2, 1980 for detail

Begin @ .006 inch/minute

Test Temp 250°F

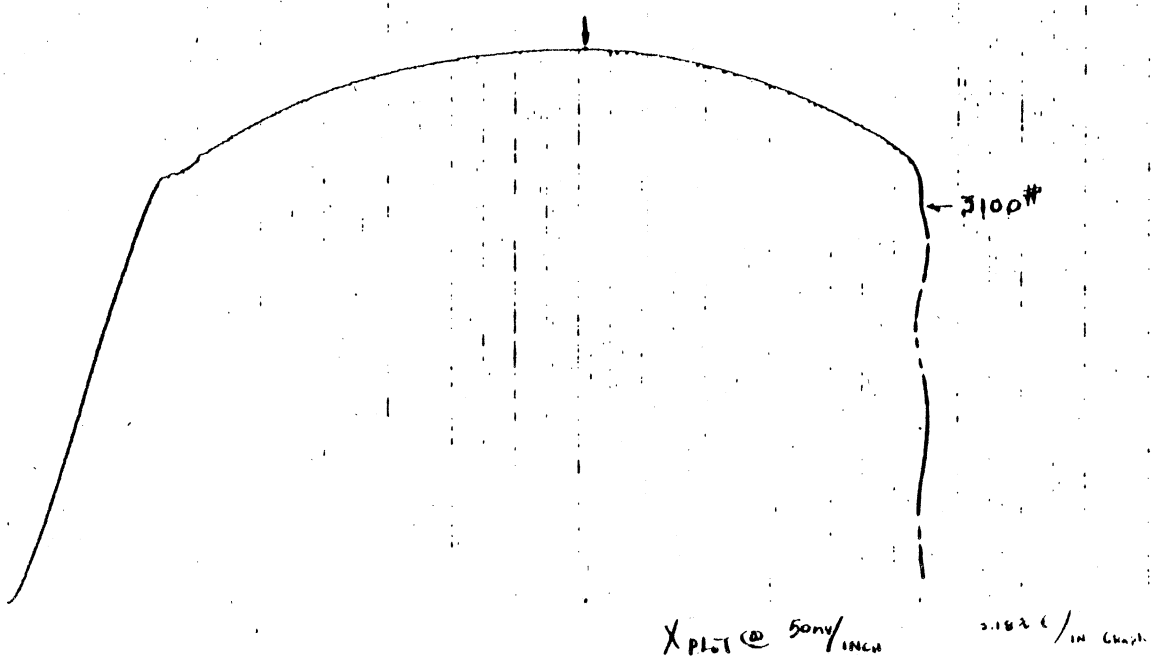

Department of Materials Sciences

TENSILE TEST DATA SHEET

T- _____ Est. U.T.S. _____ psi Project No. 02-5928-00/

R.T-9 Initial G.L. _____ in. Machine No. 50K

ure +550 °F Initial Dia. .249 in. Date 5-20-80

te _____ Initial Thickness _____ in. Initial Area .0487 in²

Initial Width _____ in.

---

p Temperature 551 °F Maximum Load 4300 lb

ttom Temperature 548 °F 0.2% Offset Load 3240 lb

nal Gage Length 1.180 in. 0.02% Offset Load _____ lb

nal Diameter .168 in. Upper Yield Point _____ lb

nal Area .0221 in.²

T.S. = $\frac{\text{Maximum Load}}{\text{Initial Area}}$ = 88.3 ~~psi~~ Ksi

2% Y.S. = $\frac{\text{0.2\% Offset Load}}{\text{Initial Area}}$ = 66.5 ~~psi~~ Ksi

02% Y.S. = $\frac{\text{0.02\% Offset Load}}{\text{Initial Area}}$ = _____ psi

per Y.S. = $\frac{\text{Upper Yield Point}}{\text{Initial Area}}$ = _____ psi

Elongation = $\frac{\text{Final G.L. - Initial G.L.}}{\text{Initial G.L.}}$ x 100 = 18.0 %

R.A. = $\frac{\text{Initial Area - Final Area}}{\text{Initial Area}}$ x 100 = 54.4 %

R. Ames

Tensile Test Harry E Clark QA 20 May 80

Spec #MT-9
May 20, 1980
Load/Strain
Temp +550°F
02-5968-001
i. .0064/mm

8.6"

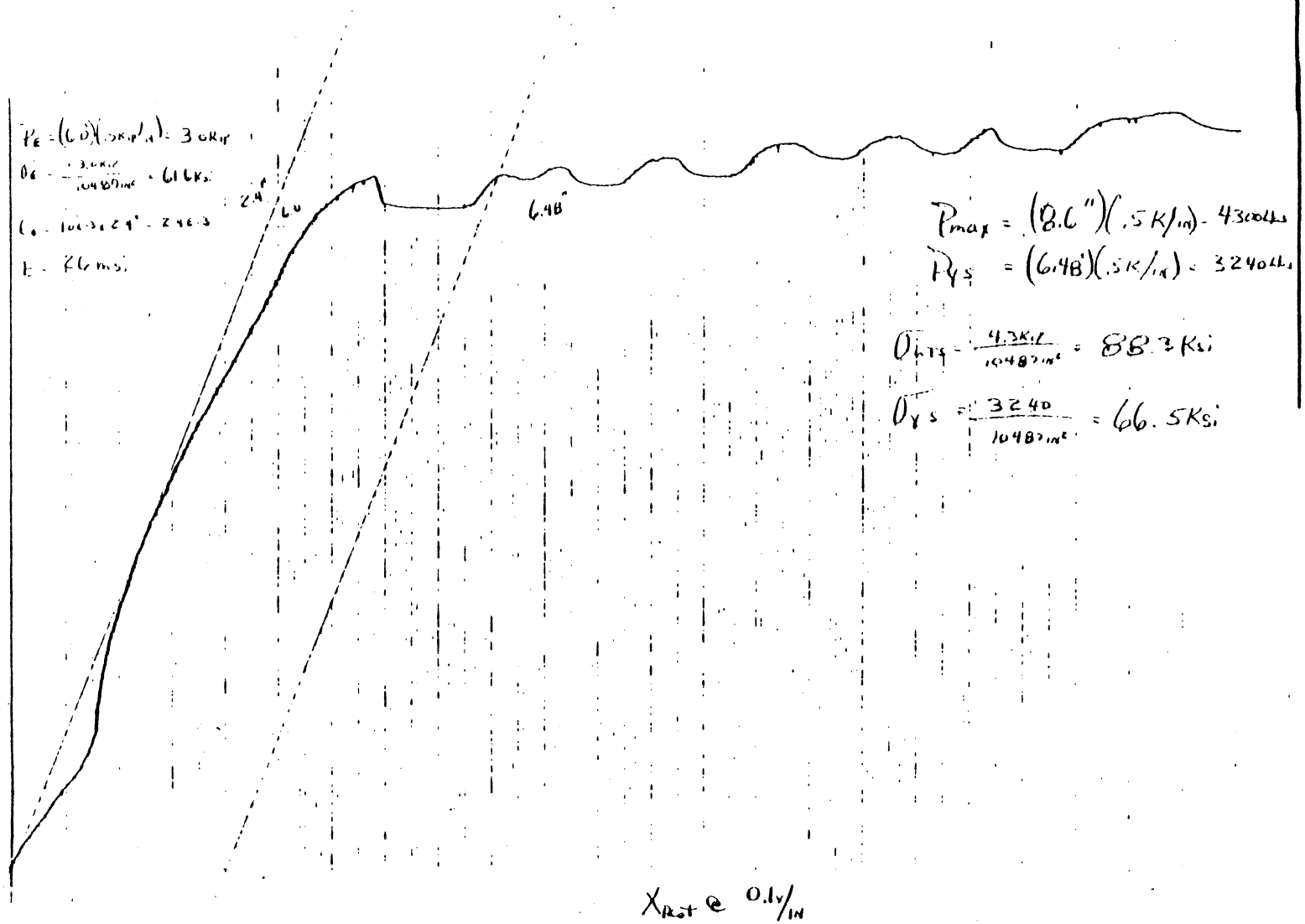

$P_E = (6.0")(.5K/_{IN}) = 3.0K_{IP}$

$\sigma_E = \frac{3.0K_{IP}}{1.048 in^2} = 61 Ksi$

$\epsilon_0 = 1.0 \times 2.4" = 2.4E{-}3$

$E = 26 msi$

$P_{max} = (8.6")(.5K/_{IN}) = 4300 Lbs$

$P_{YS} = (6.48")(.5K/_{IN}) = 3240 Lbs$

$\sigma_{UTS} = \frac{4.3K_{IP}}{1.048 in^2} = 88.3 Ksi$

$\sigma_{YS} = \frac{3240}{1.048 in^2} = 66.5 Ksi$

Spec. # MIT-9
May 20, 1980
Load/Displacement
Temp +550°F
02-502B-001
k = .006 in/in

$P_{max} = (8.6)(.5K/in) = 4.3Kip$

Elongation @ P_{max} = (.28")(.0322) = .0902 in/in

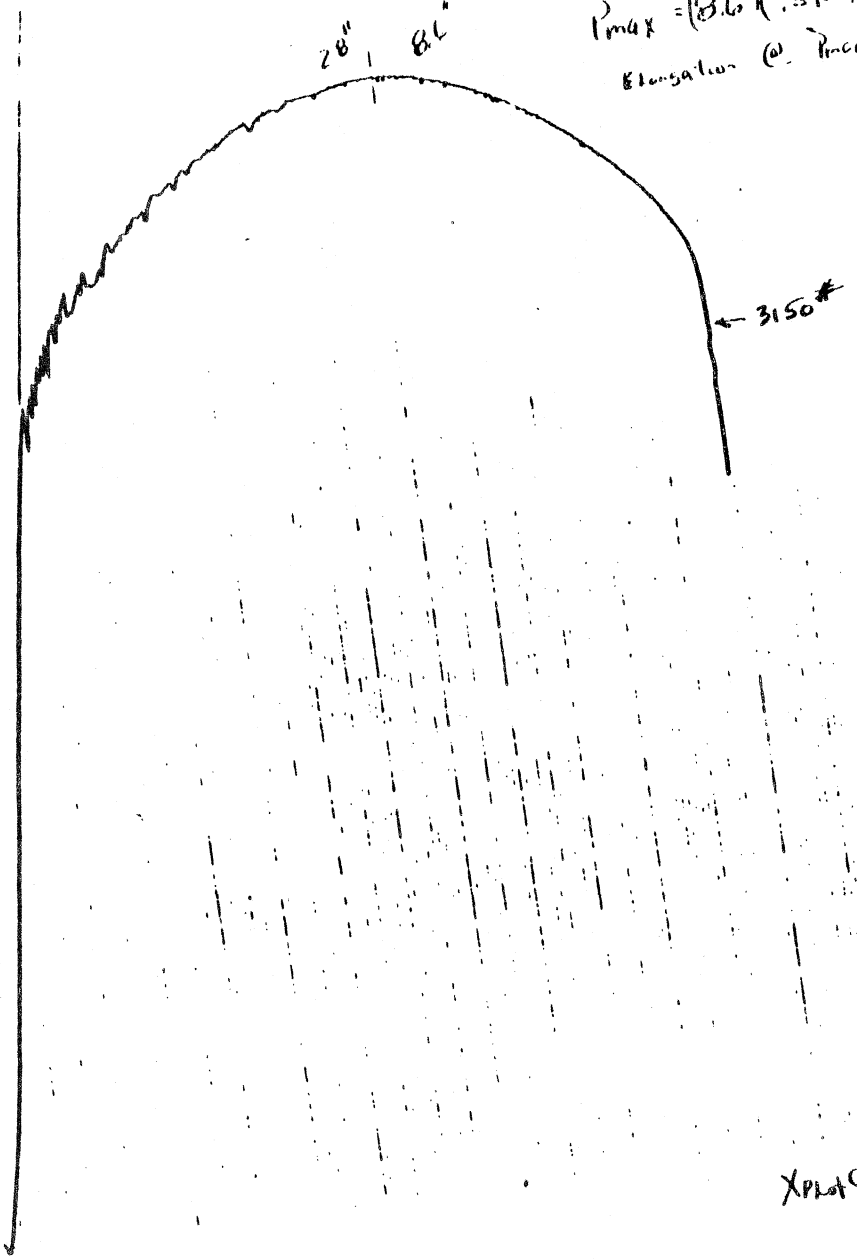

APPENDIX B

PROCEDURE FOR THE GENERATION OF ALLOWABLE PRESSURE-TEMPERATURE LIMIT CURVES FOR NUCLEAR POWER PLANT REACTOR VESSELS

PROCEDURE FOR THE GENERATION OF ALLOWABLE PRESSURE-TEMPERATURE LIMIT CURVES FOR NUCLEAR POWER PLANT REACTOR VESSELS

A. Introduction

The following is a description of the basis for the generation of pressure-temperature limit curves for inservice leak and hydrostatic tests, heatup and cooldown operations, and core operation of reactor pressure vessels. The safety margins employed in these procedures equal or exceed those recommended in the ASME Boiler and Pressure Vessel Code, Section III, Appendix G, "Protection Against Nonductile Failure."

B. Background

The basic parameter used to determine safe vessel operational conditions is the stress intensity factor, K_I, which is a function of the stress state and flaw configuration. The K_I corresponding to membrane tension is given by

$$K_{Im} = M_m \cdot \sigma_m \tag{1}$$

where M_m is the membrane stress correction factor for the postulated flaw and σ_m the membrane stress. Likewise, K_I corresponding to bending is given by

$$K_{Ib} = M_b \cdot \sigma_b \tag{2}$$

where M_b is the bending stress correction factor and σ_b is the bending stress. For vessel section thickness of 4 to 12 inches, the maximum

postulated surface flaw, which is assumed to be normal to the direction of maximum stress, has a depth of 0.25 of the section thickness and a length of 1.50 times the section thickness. Curves for M_m versus the square root of the vessel wall thickness for the postulated flaw are given in Figure 1 as taken from the Pressure Vessel Code (ref. Figure G-2114.1). These curves are a function of the stress ratio parameter σ/σ_y, where σ_y is the material yield strength which is taken to be 50,000 psi. The bending correction factor is defined as 2/3 M_m and is therefore determined from Figure 1 as well. The basis for these curves is given in ASME Boiler and Pressure Vessel Code, Section XI, "Rules for Inservice Inspection of Nuclear Power Plant Components," Article A-3000.

The Code specifies the minimum K_I that can cause failure as a function of material temperature, T, and its reference nil ductility temperature, RT_{NDT}. This minimum K_I is defined as the reference stress intensity factor, K_{IR}, and is given by

$$K_{IR} = 26777. + 1223. \exp\left[0.014493(T - RT_{NDT} + 160)\right] \qquad (3)$$

where all temperatures are in degrees Fahrenheit. A plot of this expression is given in Figure 2 taken from the Code (ref. Figure G-2010.1).

C. Pressure-Temperature Relationships

1. Inservice Leak and Hydrostatic Test

During performance of inservice leak and hydrostatic tests, the reference stress intensity factor, K_{IR}, must always be greater than

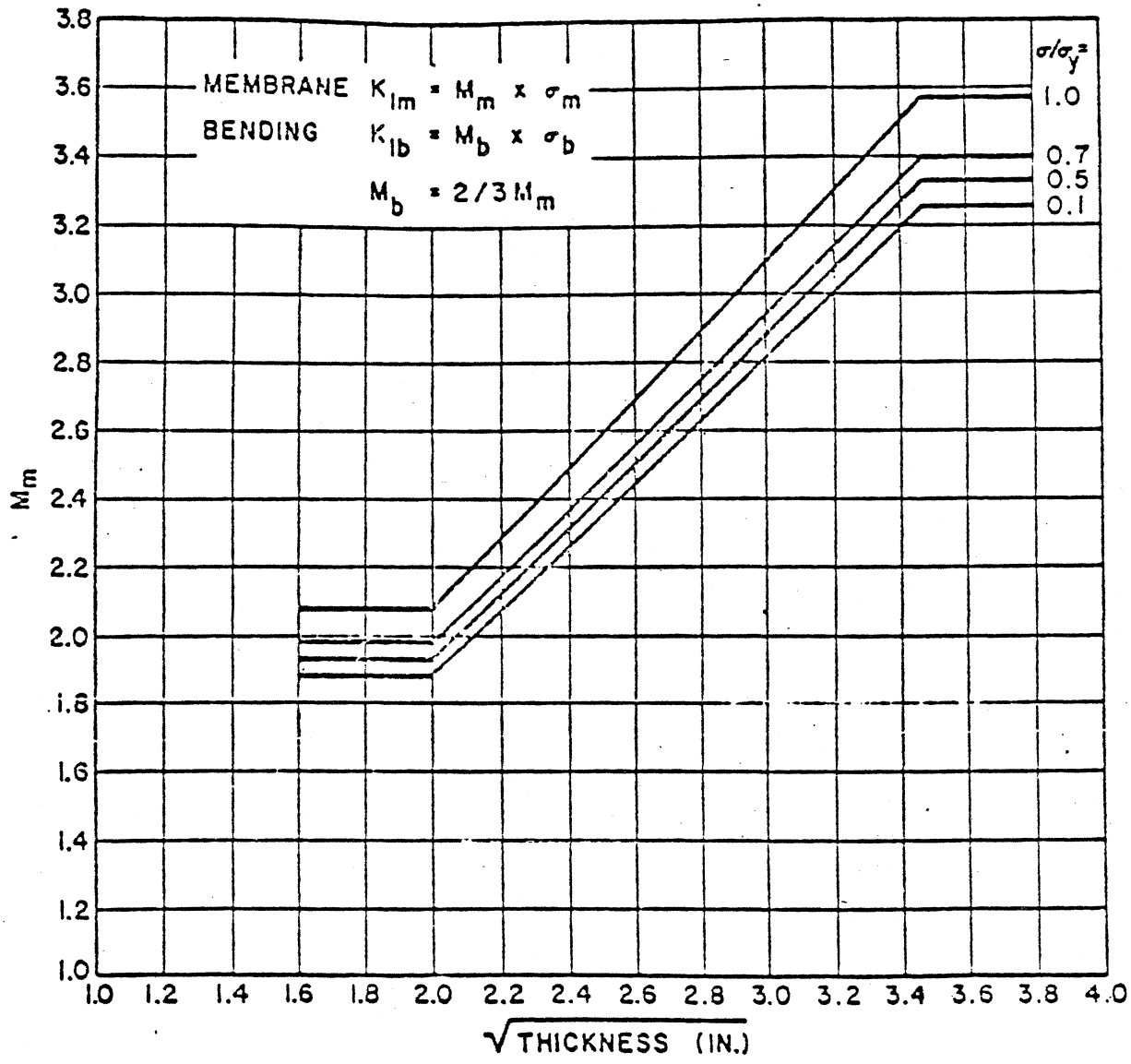

FIGURE 1. STRESS CORRECTION FACTOR

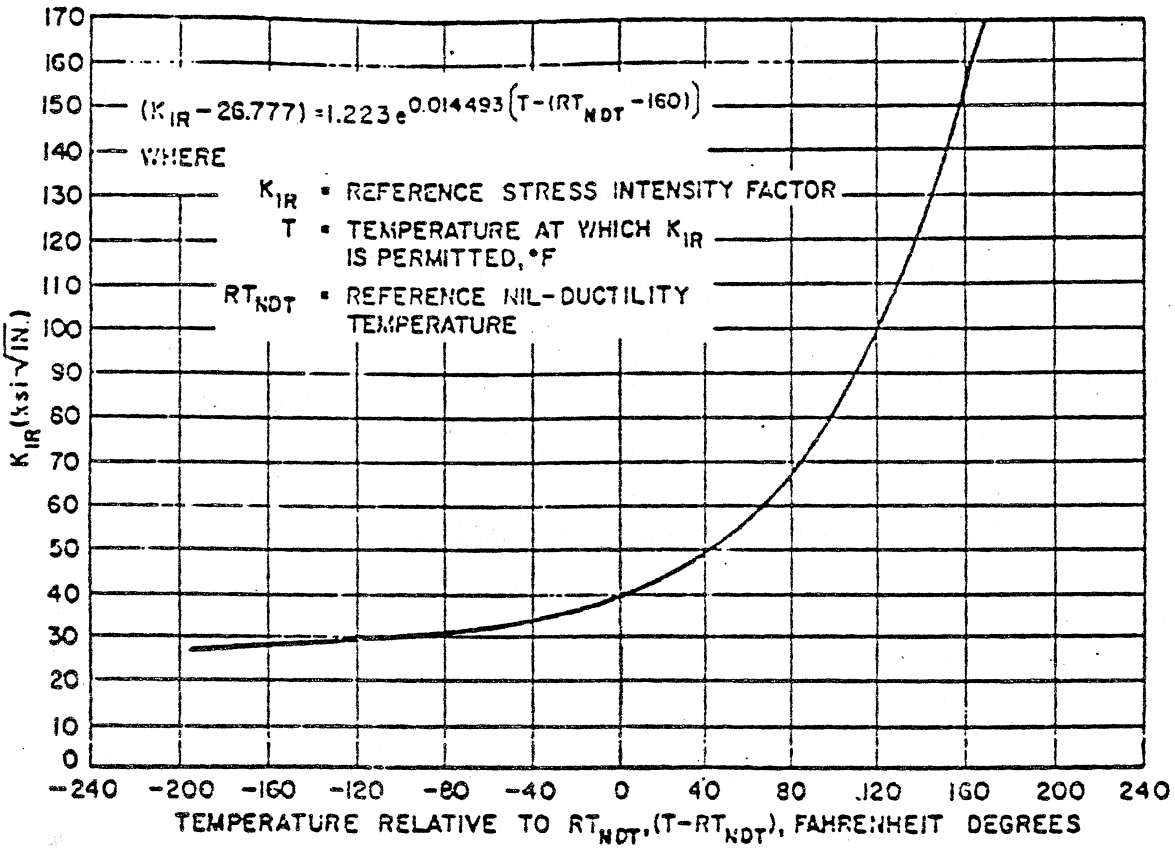

FIGURE 2. REFERENCE STRESS INTENSITY FACTOR

1.5 times the K_I caused by pressure, thus

$$1.5\ K_{Ip} < K_{IR} \tag{4}$$

or

$$1.5\ M_m\ \sigma_m < K_{IR}\,. \tag{5}$$

For a cylinder with inner radius r_i and outer radius r_o, the stress distribution due to internal pressure is given by

$$\sigma(r) = \left(\frac{r_i^2}{r_o^2 - r_i^2}\right)\left(\frac{r_o^2 + r^2}{r^2}\right)\,. \tag{6}$$

With 1/4T flaws possible at both inner and outer radial locations, i.e., at $r_{1/4} = r_i + 1/4(r_o - r_i)$ and $r_{3/4} = r_i + 3/4(r_o - r_i)$, the maximum stress will occur at the inner flaw location, thus

$$\sigma_{max} = P_o\left(\frac{r_i^2}{r_o^2 - r_i^2}\right)\left[\frac{r_o^2 + (1/4r_o + 3/4r_i)^2}{(1/4r_o + 3/4r_i)^2}\right]\,. \tag{7}$$

With the operation pressure known, i.e., P_o, we determine the minimum coolant temperature that will satisfy Equation (4) by evaluating

$$K_{IR} = 1.5\ M_m\ \sigma_{max} \tag{8}$$

and determine the corresponding coolant temperature, T, from Equation (3) for the given RT_{NDT} at the 1/4T location. For this calculation, Equation (3) takes the form

$$T = RT_{NDT}(1/4T) - 160. + 68.9988\ \ln\left[\frac{K_{IR} - 26777.}{1223.}\right]\,. \tag{9}$$

The inservice curves are generated for an operating pressure range of .96 P_o to 1.14 P_o, where P_o is the design operating pressure.

2. Heatup and Cooldown Operations

At all times during heatup and cooldown operations, the reference stress intensity factor, K_{IR}, must always be greater than the sum of 2 times the K_{Ip} caused by pressure and the K_{It} caused by thermal gradients, thus

$$2.0\ K_{Ip} + 1.0\ K_{It} < K_{IR} \tag{10}$$

or

$$2.0\ M_m\ \sigma_{max} = K_{IR} - K_{It} \tag{11}$$

where σ_{max} is the maximum allowable stress due to internal pressure, and K_{It} is the equivalent linear stress intensity factor produced by the thermal gradients. To obtain the equivalent linear stress intensity factor due to thermal gradients requires a detailed thermal stress analysis. The details of the required analysis are given in Section D.

During heatup the radial stress distributions due to internal pressure and thermal gradients are shown schematically in Figure 3a. Assuming a possible flaw at the 1/4T location, we see from Figure 3a that the thermal stress tends to alleviate the pressure stress at this point in the vessel wall and, therefore, the steady state pressure stress would represent the maximum stress condition at the 1/4T location. At

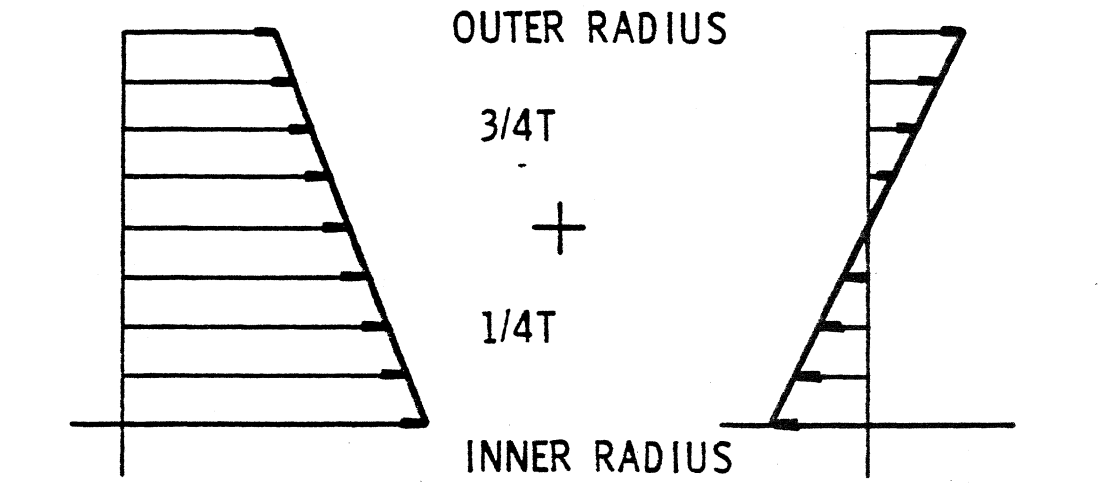

(a) Heatup

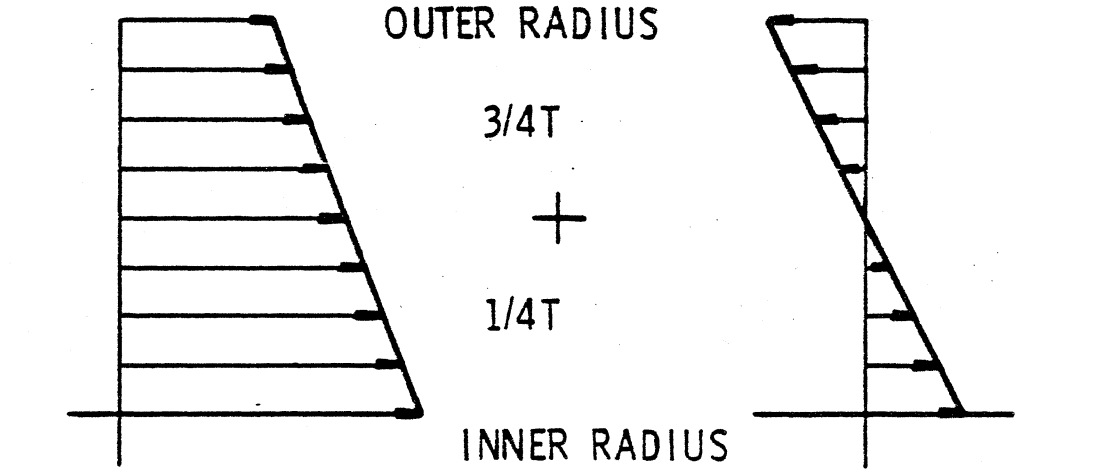

(b) Cooldown

Figure 3. Heatup and Cooldown Stress Distribution

the 3/4T flaw location, the pressure stress and thermal stress add and, therefore, the combination for a given heatup rate represents the maximum stress at the 3/4T location. The maximum overall stress between the 1/4T and 3/4T location then determines the maximum allowable reactor pressure at the given coolant temperature.

The heatup pressure-temperature curves are thus generated by calculating the maximum steady state pressure based on a possible flaw at the 1/4T location from

$$P_{max}(1/4T) = \frac{K_{IR}}{2M_m\left(\frac{r_i^2}{r_o^2 - r_i^2}\right)\left(\frac{r_o^2 + (1/4r_o + 3/4r_i)^2}{(1/4r_o + 3/4r_i)^2}\right)} \tag{12}$$

where M_m is determined from the curves in Figure 1 and K_{IR} is obtained from Equation (3) using the coolant temperature and RT_{NDT} at the 1/4T location. Here we may note that M_m must be iterated for since it is a function of the final stress ratio to yield strength (σ/σ_y).

At the 3/4T location, the maximum pressure is determined from Equation (11) as

$$P_{max}(3/4T) = \frac{K_{IR} - K_{It}}{2M_m\left(\frac{r_i^2}{r_o^2 - r_i^2}\right)\left(\frac{r_o^2 + (1/4r_i + 3/4r_o)^2}{(1/4r_i + 3/4r_o)^2}\right)} \tag{13}$$

where K_{IR} is obtained from Equation (2) using the material temperature and RT_{NDT} at the 3/4T location and K_{It} is determined from the analysis procedure outlined in Section D. M_m is determined from Figure 1.

The minimum of these maximum allowable pressures at the given coolant temperature determines the maximum operation pressure. Each heatup rate of interest must be analyzed on an individual basis.

The cooldown analysis proceeds in a similar fashion as that described for heatup with the following exceptions: We note from Figure 3b that during cooldown the 1/4T location always controls the maximum stress since the thermal gradient produces tensile stresses at the 1/4T location. Thus the steady state pressure is the same as that given in Equation (12). For each cooldown rate, the maximum pressure is evaluated at the 1/4T location from

$$P_{max}(1/4T) = \frac{K_{IR} - K_{It}}{2M_m \left(\frac{r_i^2}{r_o^2 - r_i^2}\right)\left(\frac{r_o^2 + (3/4r_i + 1/4r_o)^2}{(3/4r_i + 1/4r_o)}\right)} \qquad (14)$$

where K_{IR} is obtained from Equation (3) using the material temperature and RT_{NDT} at the 1/4T location. K_{It} is determined from the thermal analysis described in Section D.

It is of interest to note that during cooldown the material temperature will lag the coolant temperature and, therefore, the steady state pressure, which is evaluated at the coolant temperature, will initially yield the lower maximum allowable pressure. When the thermal gradients increase, the stresses do likewise, and, finally, the transient analysis governs the maximum allowable pressure. Hence a point-by-point

:omparison must be made between the maximum allowable pressures pro-
luce. by steady state analyses and transient thermal analysis to determine
he minimum of the maximum allowable pressures.

3. Core Operation

At all times that the reactor core is critical, the temperature
ıust be higher than that required for inservice hydrostatic testing, and in
ddition, the pressure-temperature relationship shall provide at least a
0°F margin over that required for heatup and cooldown operations. Thus
ıe pressure-temperature limit curves for core operation may be constructed
irectly from the inservice leak and hydrostatic test and heatup analysis
esults.

. Thermal Stress Analysis

The equivalent linear stress due to thermal gradients is obtained
om a detailed thermal analysis of the vessel. The temperature distribu-
on in the vessel wall is governed by the partial differential equation

$$\rho c T_t - K\left[(1/r)\,T_r + T_{rr}\right] = 0 \qquad (15)$$

bject to initial condition

$$T(r, 0) = T_o \,, \qquad (16)$$

d boundary conditions

$$-KT_r(r_i, t) = h\left[T_c(t) - T(r_i, t)\right] , \qquad (17)$$

and

$$T_r(r_o, t) = 0 \tag{18}$$

where

$$T_c = T_o + Rt. \tag{19}$$

ρ is the material density, c the material specific heat, K the heat conductivity of the material, h the heat transfer coefficient between the water coolant and vessel material, R the heating rate, T_o the initial coolant temperature, $T(r,t)$ the temperature distribution in the vessel, r the spatial coordinate, and t the temporal coordinate.

A finite difference solution procedure is employed to solve for the radial temperature distribution at various time steps along the heatup or cooldown cycle. The finite difference equations for N radial points, at distance Δr apart, across the vessel are:

for $1 < n < N$

$$T_n^{t+\Delta t} = \left[1 - \frac{\Delta t K}{\rho c (\Delta r)^2}\left(2 + \frac{\Delta r}{r_n}\right)\right] T_n^t + \frac{\Delta t K}{\rho c (\Delta r)^2}\left[\left(1 + \frac{\Delta r}{r_n}\right) T_{n+1}^t + T_{n-1}^t\right], \tag{20}$$

for $n = 1$

$$T_1^{t+\Delta t} = \left[1 - \frac{\Delta t K}{\rho c (\Delta r)^2}\left(1 + \frac{\Delta r}{r_1}\right) - \frac{\Delta t h}{\rho c (\Delta r)}\right] T_1^t + \frac{\Delta t K}{\rho c (\Delta r)^2}\left[\left(1 + \frac{\Delta r}{r_1}\right) T_2^t + \frac{\Delta r h}{K} T_c^t\right], \tag{21}$$

and for n = N

$$T_N^{t+\Delta t} = \left[1 - \frac{\Delta t K}{\rho c (\Delta r)^2}\right] T_N^t + \frac{K \Delta t}{\rho c (\Delta r)^2} T_{N-1}^t \quad . \tag{22}$$

For stability in the finite difference operation, we must choose Δt for a given Δr such that both

$$\frac{\Delta t K}{\rho c (\Delta r)^2} \left(2 + \frac{\Delta r}{r_1}\right) \leq 1 \tag{23}$$

and

$$\frac{\Delta t K}{\rho c (\Delta r)^2} \left(1 + \frac{\Delta r}{r_1}\right) + \frac{\Delta t h}{\rho c (\Delta r)} \leq 1 \tag{24}$$

are satisfied. These conditions assure us that heat will not flow in the direction of increasing temperature, which, of course, would violate the second law of thermodynamics.

Since a large variation in coolant temperature is considered, the dependence of $(K/\rho c)$, K, and h on temperature is included in the analysis by treating these as constants only during every 5 °F increment in coolant temperature and then updating their values for the next 5 °F increment. The dependence of $(K/\rho c)$ called the thermal diffusivity and K, the thermal conductivity, can be determined from the ASME Boiler and Pressure Vessel Code, Section III, Appendix I - Stress Tables. A linear regression analysis of the tabular values resulted in the following expressions:

$$K(T) = 38.211 - 0.01673 * T \ (BTU/HR\text{-}FT\text{-}^\circ F) \tag{25}$$

and

$$k(T) = (K/\rho c) = 0.6942 - 0.000432 * T \ (FT^2/HR) \tag{26}$$

where T is in degrees Fahrenheit.

The heat transfer coefficient is calculated based on forced convection under turbulent flow conditions. The variables involved are the mean velocity of the fluid coolant, the equivalent (hydraulic) diameter of the coolant channel, and the density, heat capacity, viscosity, and thermal conductivity of the coolant. For water coolant, allowance for the variations in physical properties with temperature may be made by writing*

$$h(T) = 170(1 + 10^{-2} * T - 10^{-5} * T^2) \ v^{0.8}/D^{0.2} \tag{27}$$

where v is in ft/sec, D in inches, the temperature is in °F, and h is in Btu/hr-ft^2-°F. The values for the heat-transfer coefficient given by this relationship are in good agreement with those obtained from the Dittus-Boelter equation for temperatures up to 600°F. The mean velocity of the coolant, v, is generally given in terms of the effective coolant flow rate Q (Lbm/hr) and effective flow area A (ft^2). Given the relationship

$$\rho(T) = 62.93 - 0.48 \times 10^{-2} * T - 0.46 \times 10^{-4} * T^2 \tag{28}$$

for the density of water as a function of temperature, the mean velocity of the coolant is obtained from

$$v = Q/(3600 * \rho(T) * A) \ . \tag{29}$$

---

* Glasstone, S., Principles of Nuclear Reactor Engineering, D. Van Nostrand Co., Inc., New Jersey, pp. 667-668, 1960.

The thermal stress distribution is calculated from

$$\sigma_T(r,t) = \frac{\alpha E}{1-\nu}\left[\frac{1}{r^2}\int_{r_i}^{r} T(r,t)\,r\,dr - T(r,t) + \frac{1}{r^2}\left(\frac{r^2+r_i^2}{r_o^2-r_i^2}\right)\int_{r_i}^{r_o} T(r,t)\,r\,dr\right] \quad (30)$$

where α is the coefficient of thermal expansion (in/in °F), E is Young's modulus, and ν is Poisson's ratio. This expression can be obtained from Theory of Elasticity by Timoshenko and Goodier, pp. 408-409, when imposing a zero radial stress condition at the cylinder inner and outer radius. Poisson's ratio is taken to be constant at a value of 0.3 while α and E are evaluated as a function of the average temperature across the vessel

$$T_{avg} = \frac{2}{(r_o^2 - r_i^2)}\int_{r_i}^{r_o} T(r)\,r\,dr \quad . \quad (31)$$

The dependence of the coefficient of thermal expansion on temperature is taken to be

$$\alpha(T) = 5.76 \times 10^{-6} + 4.4 \times 10^{-9} * T \quad (32)$$

and the dependence of Young's modulus on temperature is taken to be

$$E(T) = 27.9142 + 2.5782 \times 10^{-4} * T - 6.5723 \times 10^{-6} * T^2 \quad (33)$$

as obtained from regression analysis of tabular values given in Section III, Appendix I of the ASME Boiler and Pressure Vessel Code.

The resulting stress distribution given by Equation (30) is not linear; however, an equivalent linear stress distribution is determined from the resulting moment. The moment produced by the nonlinear

stress distribution is given by

$$M(t) = b\int_{r_i}^{r_o} \sigma_T(r,t)\, r\, dr \tag{34}$$

where b is a unit depth of the vessel. Here we note that the moment is a function of time, i.e., coolant temperature via $T_c = To + Rt$. For a linear stress distribution we have that

$$\sigma_{max} = \frac{Mc}{I} \tag{35}$$

where σ_{max} is the maximum outer fiber stress, c the distance from the neutral axis, taken to be $(r_o - r_i)/2$, and I the section area moment of inertia which is given by

$$I = \frac{bh^3}{12} = \frac{b(r_o - r_i)^3}{12} \tag{36}$$

Combining these expressions results in the equivalent linear stress due to thermal gradients

$$\sigma_{max} = \sigma_{bt} = \frac{6}{(r_o - r_i)^2}\int_{r_i}^{r_o} \sigma_T(r,t)\, r\, dr \tag{37}$$

The thermal stress intensity factor K_{It} is then defined as

$$K_{It} = M_b\, \sigma_{bt} \tag{38}$$

where M_b is determined from the curves given in Figure 1 wherein $M_b = 2/3\ M_m$. It is of interest to note that a sign change occurs in the stress calculations during a cooldown analysis since the thermal gradients

produce compressive stresses at the vessel outer radius. This sign change must then be reflected in the K_{It} calculation for the cooldown analysis.

Normalized temperature and thermal stress distributions during a typical reactor heatup are given in Figure 4. The radial temperature is shown normalized with respect to the average temperature, T_{avg}, by

$$T = \frac{T - T_{avg}}{(T - T_{avg})_{max}} \quad . \tag{39}$$

The thermal stress and equivalent linearized stress, as calculated by Equations (30) and (37), are normalized with respect to the maximum thermal stress. Here we note that the actual thermal stress at the 3/4T location is considerably less than the maximum equivalent linear stress which yields additional safety margins during the heatup cycle. Similar temperature and thermal stress distributions are developed during cooldown. The trends are nearly identical as those shown in Figure 4 when the inner and outer vessel locations are reversed with the 1/4T location becoming the critical point.

E. Example Calculations

The following example is based on a reactor vessel with the following characteristics:

Inner Radius	=	82.00 in.	(r_i)
Outer Radius	=	90.00 in.	(r_o)
Operating Pressure	=	2250 psig	(P_o)

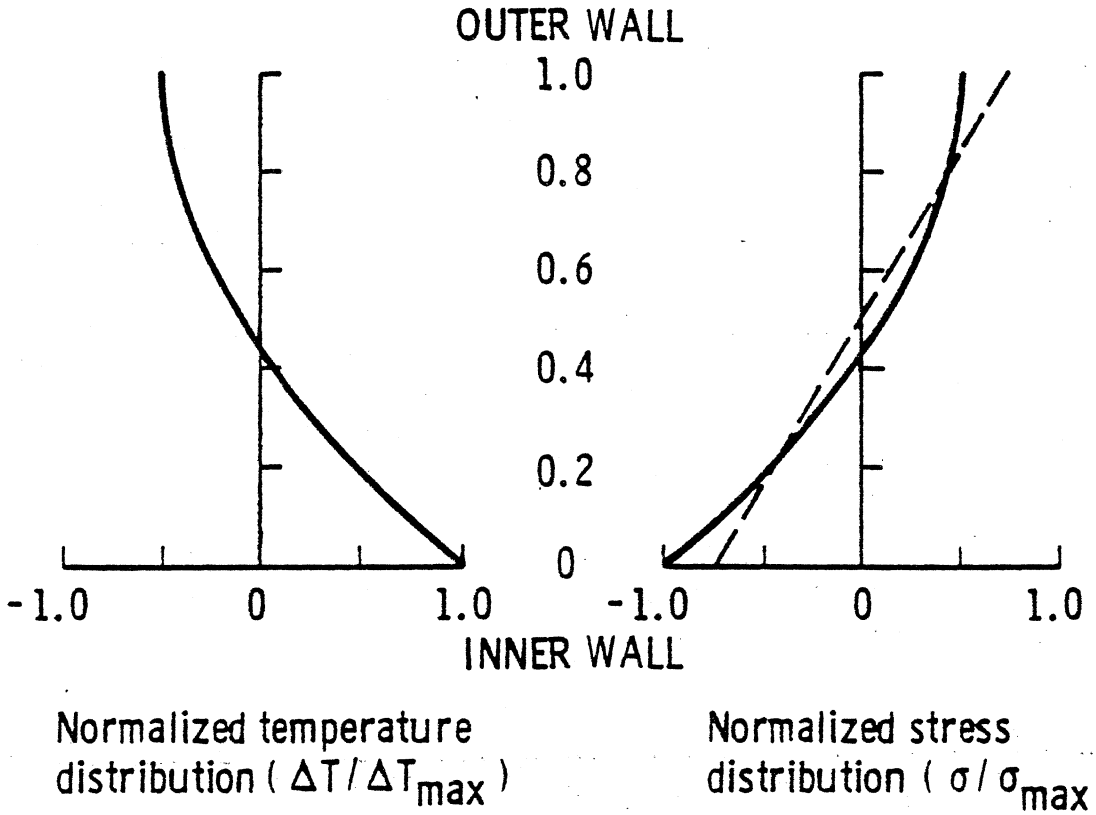

Figure 4. Typical Normalized Temperature and Stress Distribution During Heatup

Initial Temperature	=	70°F	(T_o)
Final Temperature	=	550°F	(T_f)
Effective Coolant Flow Rate	=	100×10^6 Lbm/hr	(Q)
Effective Flow Area	=	20.00 ft^2	(A)
Effective Hydraulic Diameter	=	10.00 in.	(D)
RT_{NDT} (1/4T)	=	200°F	
RT_{NDT} (3/4T)	=	140°F	

In the thermal stress analysis 21 radial points were used in the finite difference scheme. Going from 70°F to the final temperature of 550°F, approximately 12,000 time (temperature via T = To + Rt) steps were required in the thermal analysis for the 100°F/hr heatup rate. The results of the computation are shown in Figures 5 through 9.

Figure 5 gives the reference stress intensity factor, K_{IR}, as a function of temperature indexed to RT_{NDT} (1/4T). For the steady state analysis, K_{IR} is converted directly to allowable pressure via Equation 12.

During the heatup and cooldown thermal analyses the material temperature at the 1/4T and 3/4T and thermal stress intensity factors K_{It} are required to compute allowable pressure via Equations (13) and (14). The material temperatures versus coolant temperature during the 100°F/hr heatup and cooldown analyses are given in Figure 6. These temperatures allow computation of the corresponding reference stress intensity factors, K_{IR} (3/4T) and K_{IR} (1/4T). Figure 7 gives the corresponding thermal stress intensity factor at the 3/4T and 1/4T locations as a function of coolant temperature.

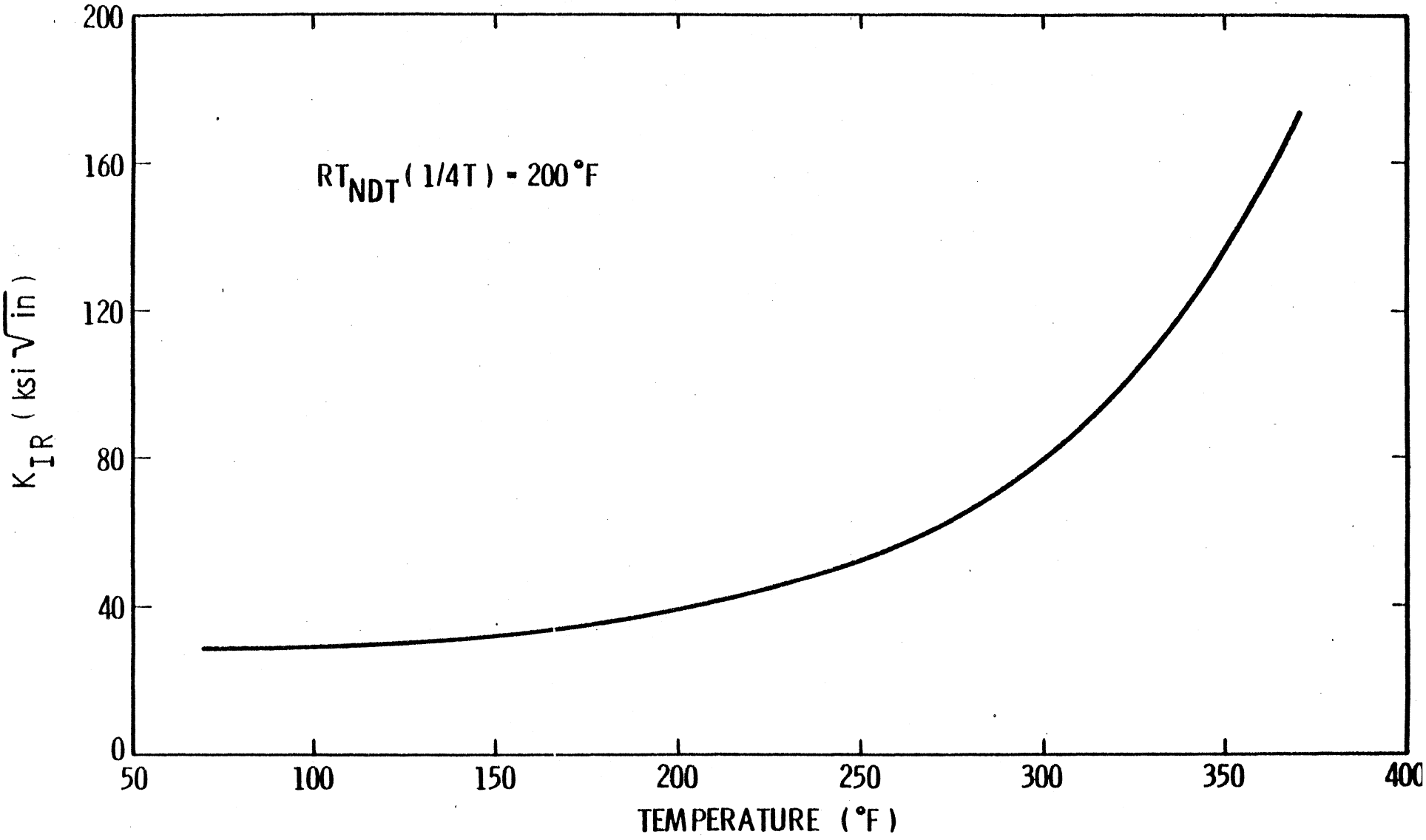

Figure 5. Reference Stress Intensity Factor as a Function of Temperature Indexed to RT_{NDT} (1/4T)

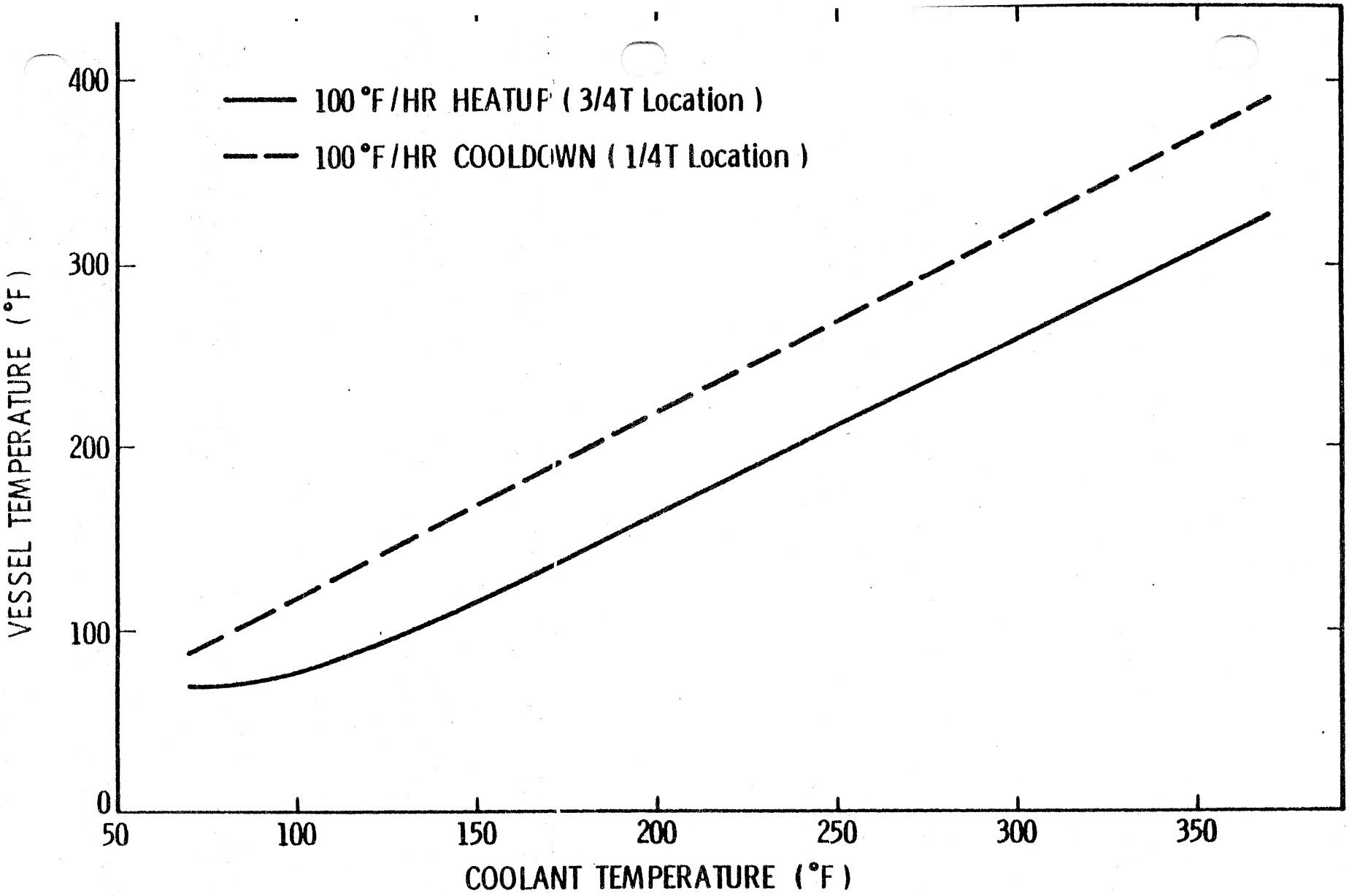

Figure 6. Vessel Temperature at 1/4T and 3/4T Locations as a Function of Coolant Temperature

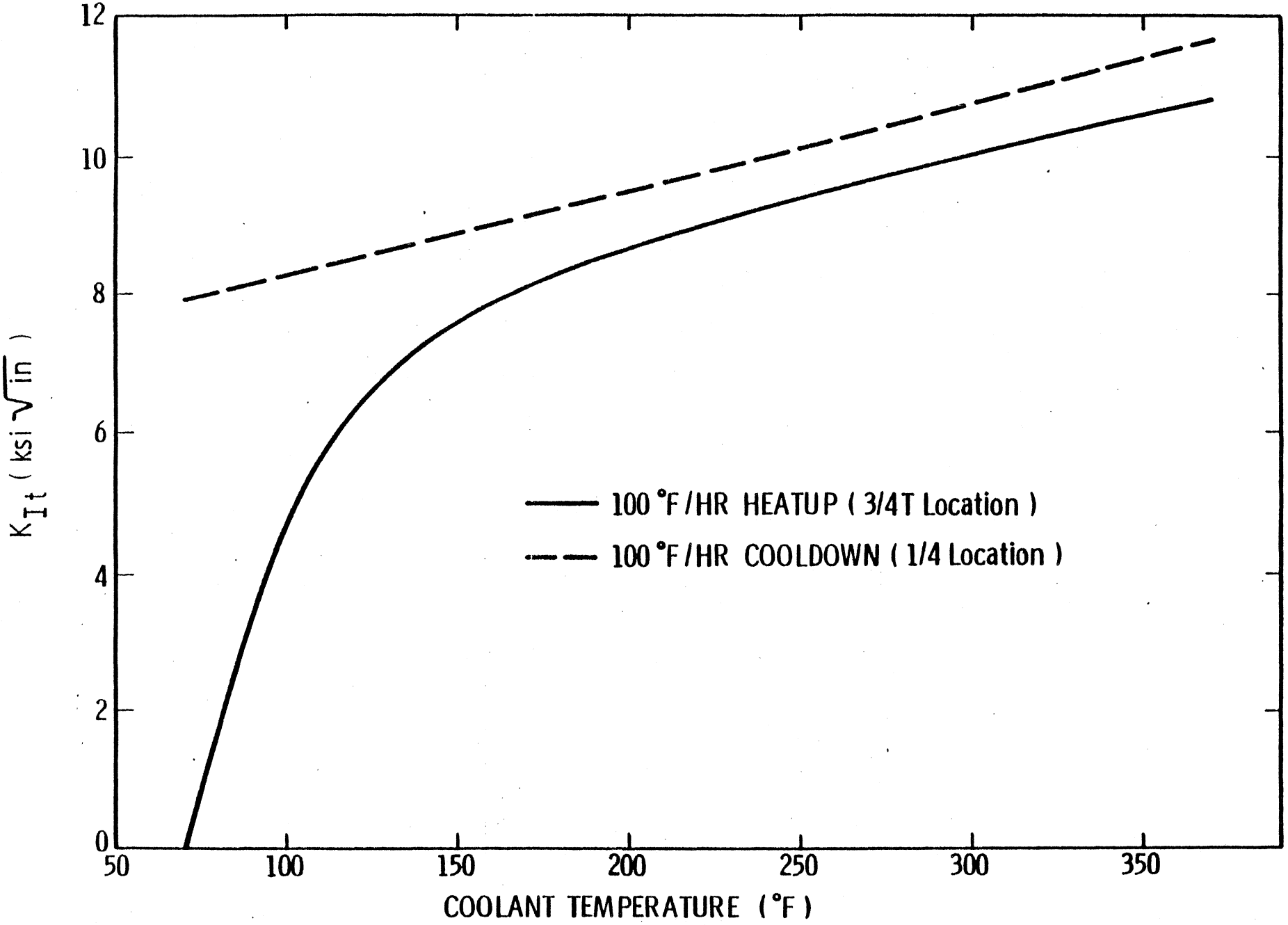

Figure 7. Thermal Stress Intensity Factor at 3/4T and 1/4T Locations as a Function of Coolant Temperature

Figures 8 and 9 demonstrate the construction of the allowable composite pressure and temperature curves for the 100°F/hr heatup and cooldown rates. The composite curves represent the lower bound of the thermal and steady state curves with the addition of margins of +10°F and -60 psig for possible instrumentation error. Figure 8 also shows the leak test limit, corrected for instrument error, as obtained from Equation (9). The limit points are at the operating pressure 2250 psig and at 2475 psig which corresponds to 1.1 times the operating pressure. The criticality limit is also shown in Figure 8 and is constructed by providing for a 40°F margin over that required for heatup and cooldown and by requiring that the minimum temperature be greater than that required by the leak test limit.

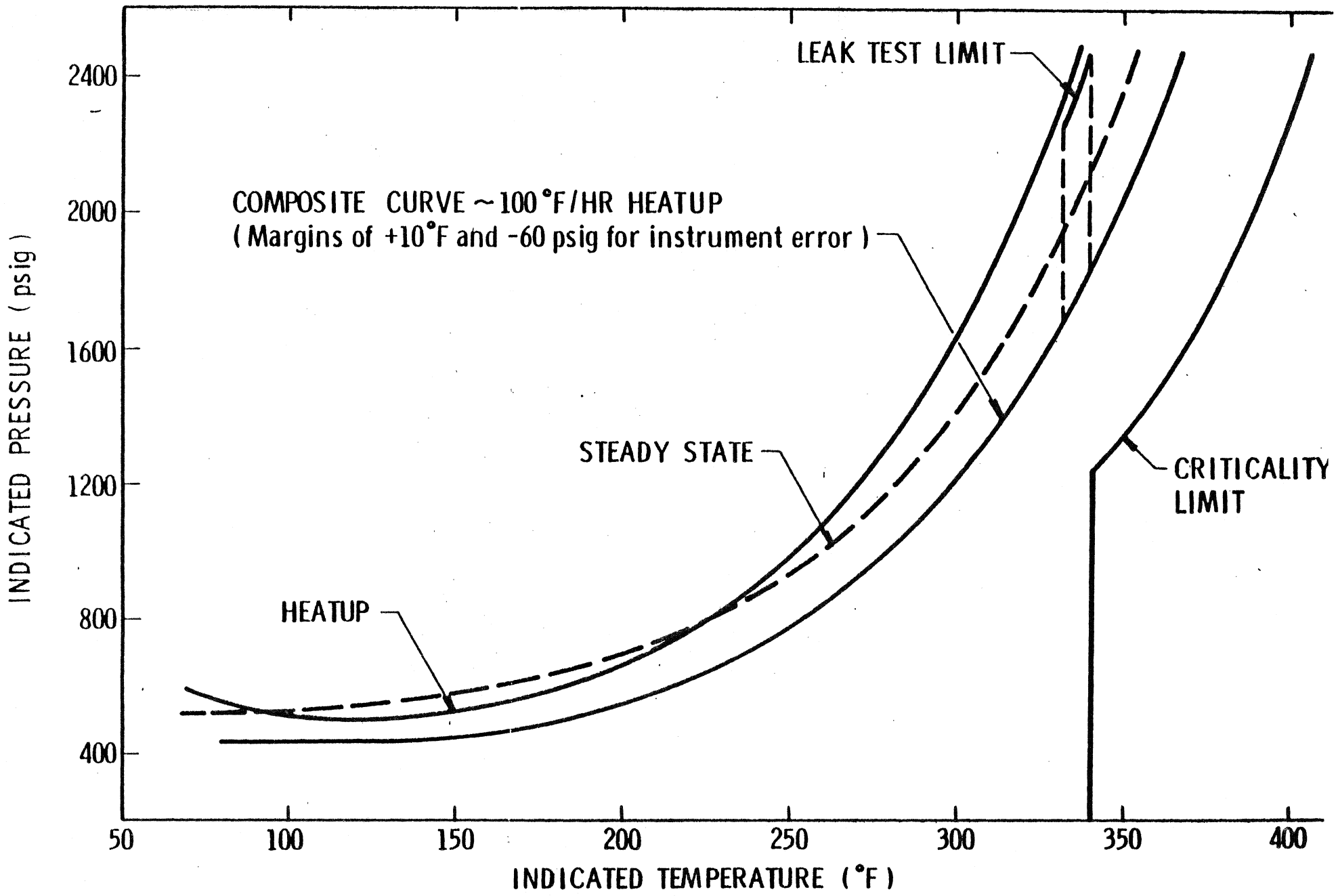

Figure 8. Pressure-Temperature Curves for 100 °F/Hr Heatup

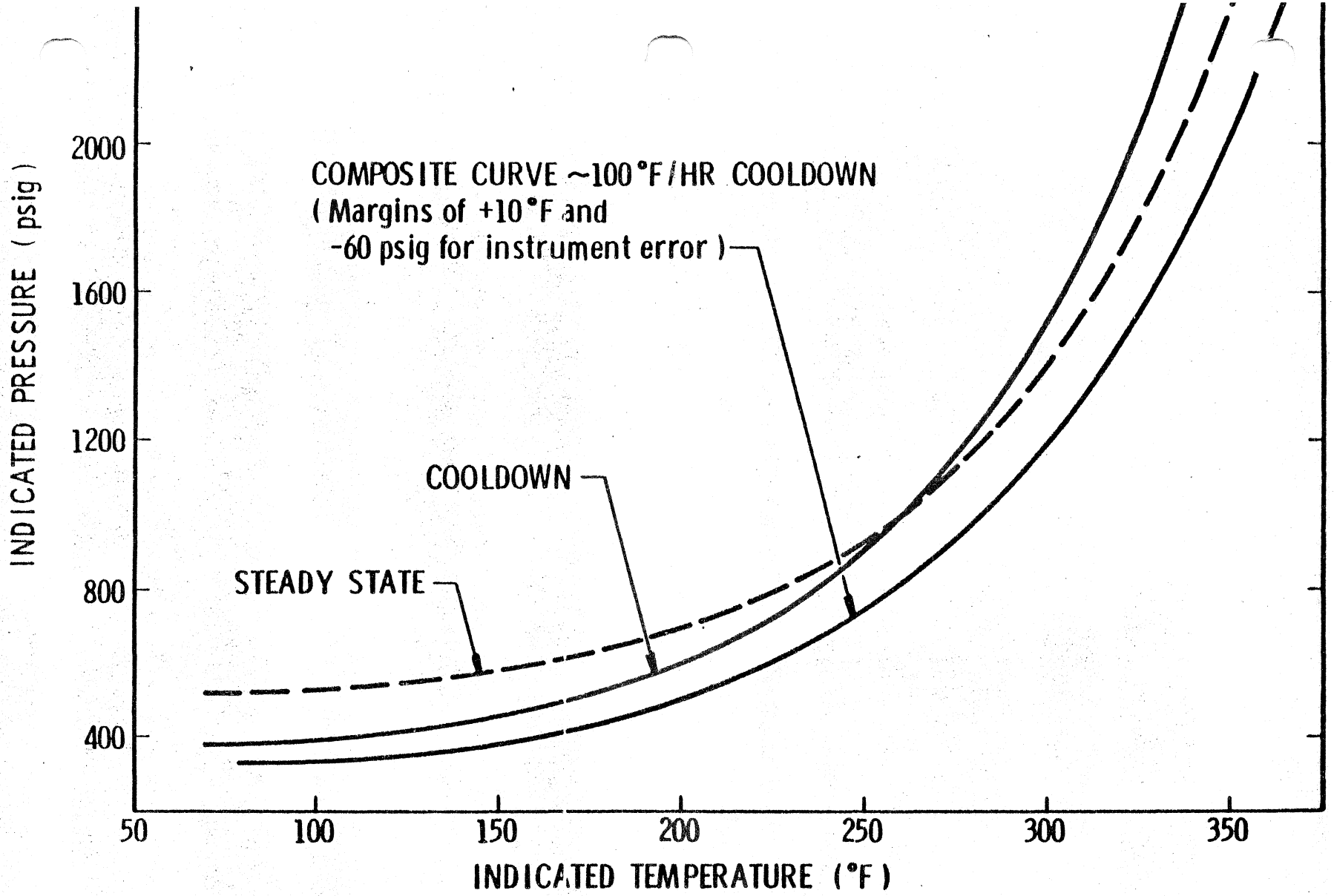

Figure 9. Pressure - Temperature Curves for 100°F/Hr Cooldown

Plate C5521-2	PCK201	LT/TL	T
Weld	WCK201	TL	—
Hoz	HCK201	—	

SWRI-02-5928

Chem_pr	N/A - dupe
Heat_pr	N/A - dupe
Hlst_lst	N/A - dupe
Haz_pr	N/A - dupe
Reac_pr	✓ - add_u3 (check prev. for unique)
Reac_lst	N/A - dupe
Ref_lst	✓ - add - u3
Ref_titl	✓ - add - u3
Shft_pr	✓ - add
Spec_lst	N/A - dupe to wcap-8512
Ten_pr	✓ - add
Weld_pr	N/A -
Raw_c_pr	✓ - add irrad. only
Cv_Rf_pr	✓ - add

Power-time	✓		
WOL	✓		
P-T	✓	p. 34, 36, 37	w-38
Lead	✓		
P_T_Reac	N/A		